Received: 29 July 2019 | Revised: 29 December 2019 | Accepted: 5 January 2020

DOI: 10.1002/gj.3757

SPECIAL ISSUE ARTICLE

WILEY

Leaf temperature and its dependence on atmospheric CO_2 and leaf size

Wilfried Konrad[1,2] | Gabriel Katul[3] | Anita Roth-Nebelsick[4]

[1]Department of Geosciences, University of Tübingen, Tübingen, Germany

[2]Institute of Botany, Technical University of Dresden, Dresden, Germany

[3]Nicholas School of the Environment, Duke University, Durham, North Carolina

[4]State Museum of Natural History Stuttgart, Stuttgart, Germany

Correspondence
Wilfried Konrad, Department of Geosciences, University of Tübingen, Tübingen, Germany.
Email: wilfried.konrad@uni-tuebingen.de

Funding information
Volkswagen Foundation, Grant/Award Numbers: 87139, 87160, 87160-1

Peer Review
The peer review history for this article is available at https://publons.com/publon/10.1002/gj.3757.

Handling Editor: T. Utescher

There is general concern that the rapid increase in atmospheric CO_2 concentration will lead to reduced stomatal conductance and subsequent increases in leaf temperature. Such an increase in leaf temperature is expected to adversely impact a plethora of processes connected to leaf metabolism and microbial/fungal communities on leaves. A model is proposed that combines the leaf energy balance with leaf gas exchange and photosynthesis to explore such issues. The model represents a hybrid ecological/physiological approach described by systems of equations based on steady-state leaf-gas exchange theories and leaf energy/radiation balance, equilibrium thermodynamics within the leaf, stomatal data, and atmospheric CO_2 concentration. The model allows separating air from leaf temperatures thereby permitting exploration of the dependence of leaf cooling or heating for any combination of environmental conditions (e.g., wind velocity, atmospheric humidity, and atmospheric CO_2 level), anatomic leaf properties (e.g., leaf size), and physiologic quantities (e.g., assimilation rate and transpiration rate). The model permits to distinguish whether leaf cooling or heating is to be expected if these parameters are varied. Based on model calculations, it is shown that leaf temperature is far more impacted by leaf size or wind speed than reduction in stomatal conductance caused by elevated atmospheric CO_2. The model results are consistent with measurements of leaf cooling and heating.

KEYWORDS
atmospheric CO_2, gas exchange, leaf cooling, leaf energy exchange, leaf heating, leaf size

1 | INTRODUCTION

Plants are affected by changes in atmospheric CO_2 levels directly and indirectly. Being the substrate of photosynthesis, atmospheric CO_2 affects plants directly through leaf gas exchange that is driven by the gas concentration difference between leaf interior and exterior. A rise in exterior CO_2 concentration, termed C_a throughout the rest of the text, does not necessarily lead to a proportional rise in photosynthesis, because the assimilation rate is affected by temperature, saturation kinetics of the involved biochemical apparatus, and leaf conductance (which are partially interdependent). The overall leaf conductance, g, offering the diffusional pathway connecting CO_2 source (atmosphere) and sink (mesophyll), consists of a mesophyll conductance, a stomatal conductance g_s, and an aerodynamic conductance. By and large, g_s is presumed to be the most restrictive though the remaining two conductances can be restrictive under certain conditions, such as low wind speed or soil moisture stress states. It can be generally observed that g_s responds inversely to C_a to match atmospheric supply with sink demand, by decreasing stomatal aperture and/or number of stomata (Ainsworth and Rogers, 2007; De Boer et al., 2011; Franks et al., 2013, 2014; Lammertsma et al., 2011; Leakey et al., 2009; Wagner et al., 1996). Because the stomatal pathway allows water vapour to escape

from the leaf interior, photosynthesis and transpiration are coupled through g_s. Stomatal conductance g_s is regulated by two mechanisms: the guard cells that can vary stomatal aperture on short time scales (of the order of minutes to tens of minutes), whereas the maximum value of g_s is limited by stomatal density and size and thus changes on much longer time scales (e.g., from one growing season to the next and/or even longer time scales defined by evolutionary adaptation).

Additionally, increases in global atmospheric CO_2 concentrations influence photosynthesis indirectly, via increases in global air temperatures. Temperature controls numerous leaf metabolic processes thereby exerting controls on photosynthesis. Moreover, both leaf assimilation rate, A, and leaf transpiration rate, E, depend on temperature: A shows an optimum value, A_{opt}, at the related temperature T_{opt}, whereas the saturation vapour pressure increases monotonically with increasing temperature as described by the Clausius–Clapeyron equation. Processes at the leaf-level are, however, not dependent on air temperature T_a but on leaf temperature T_l. The T_l can be different from T_a due to several processes that exchange energy between the leaf surface and the atmosphere (De Boeck, Van De Velde, De Groote, and Nijs, 2016; Jones, 2013; Smith, 1978; Nobel, 2005). Leaf energy exchange is affected by gas exchange because transpiration within the leaf consumes heat that is then "exported" to the atmosphere as latent heat (causing "evaporative cooling"). This process contributes substantially to the energy budget of the leaf (Gates, 1968; Jones, 1999, 2013).

Under elevated C_a (and otherwise identical conditions), a decrease in g_s is thus expected to reduce evaporative cooling thereby enhancing the risk for plants to reach a critically high T_l when T_a is also high. Rising T_l due to elevated C_a in the future was suggested to be particularly detrimental for tropical vegetation by causing leaf temperatures to exceed T_{opt} (Doughty and Goulden, 2008). Higher T_l due to less evaporative cooling would also affect not only plants. For example, for insects living close to the leaf surface, any changes in average T_l would mean a substantial altering of their typical habitat conditions (Pincebourde and Casas, 2006; Pincebourde and Woods, 2012; Zavala, Nabity, and DeLucia, 2013).

The importance of evaporative cooling depends on leaf size because the thickness of the leaf boundary layer increases with the size of the object (Schuepp, 1993). Increases in boundary layer thickness particularly impedes conductive and convective cooling (heat transfer by heat conduction and air currents, respectively) as well as gas exchange. Under identical wind conditions, small leaves experience a thinner boundary layer than larger leaves. This difference is due to the fact that as air encounters a leaf surface, a boundary layer is initiated at this intersection point and begins to develop and grow on the leaf surface along the local wind direction. Smaller leaf dimensions prevent this growing boundary layer to become too thick resulting in average boundary layer thicknesses that are smaller when compared to larger leaves for the same incident wind speed. The thinner boundary layer makes conductive and convective cooling more effective. Hence, small leaves, in effect, are less dependent on transpiration for a cooling mechanism (Gates, 1968; Huang, Chu, Hsieh, Palmroth, and Katul, 2015). Elevated C_a, particularly high levels of 1,000 ppm and more, as are anticipated for the end of this century in worst case scenarios (Nakicenovic et al., 2000), appears especially problematic for large leaves with respect to leaf overheating. In fact, high C_a conditions of the past were suggested to have suppressed the evolution of megaphylls during early stages of land plant evolution (Beerling, Osborne, and Chaloner, 2001). The absolute area of a leaf, however, is less crucial for boundary layer thickness than leaf shape along the predominant wind direction. This is because the thickness of the boundary layer does not depend on the total area but rather on the "characteristic dimension," l_c (Nobel, 2005; Vogel, 2009), over which the boundary layer develops. Leaves with the same area can thus show different heat exchange characteristics depending on leaf shape (Roth-Nebelsick, 2001; Vogel, 1968). For leaves with $l_c \lesssim 2$cm, heat transfer is dominated by convection (Gates, 1968).

The interrelation between g, A, E, T_a, T_l, l_c, and wind speed, v_w, are complex and mutually intertwined, leading to counteracting and sometimes counter-intuitive effects. As an illustration, consider the following situation: Supposing that T_l and vapour pressure difference (VPD) between the leaf interior (assumed saturated) and the atmosphere change slowly. A sudden drop in g_s will lead to a lower transpiration rate E, meaning that fewer water molecules are vaporized, producing less evaporative cooling. Consequently, the leaf temperature T_l increases, leading to a higher saturation vapour pressure of water molecules within the leaf. This, in turn, leads to a higher VPD between leaf interior and the atmosphere (assuming that atmospheric temperature and humidity remain constant), thereby enhancing transpiration. Since transpiration rate E is proportional to the product of leaf conductance g and to VPD, it is not possible to predict which of the two rivalling effects—a decrease in g due to stomatal closure or an increase in VPD because of elevated leaf temperature—dominates in the end, unless a quantitative theory encompassing both effects is at hand. Even in this example, another complication arises because g is related to assimilation rate A, which in turn varies with T_l, as already mentioned.

Finally, variation of v_w can generate other counter-intuitive effects: Increasing wind speed reduces the thickness of the boundary layer, thereby increasing leaf conductance g. Assuming as above that T_l and VPD react sluggishly, transpiration rate increases whereupon evaporative cooling is intensified. Thus, T_l begins to drop, water vapour saturation pressure within the leaf and VPD follow, and E decreases somewhat. Again, E is affected by two competing mechanisms, and a quantitative theory is required to assess the net effect. Observations reviewed elsewhere (Grace, 1988; Huang et al., 2015) show that increased wind speed can actually decrease transpiration rate for certain environmental conditions. In fact, higher wind speed can increase water use efficiency (WUE = A/E) just because of stomatal closure under these circumstances (Schymanski & Or, 2016).

Taking all these relations together, it appears difficult to predict how changing C_a might affect T_l in isolation. Because T_l is an essential ecophysiological quantity, it is, however, desirable to evaluate possible mutual interrelations with C_a, and such an analysis cannot ignore the role of l_c. These issues motivate the development of the mathematical model to be described here. In particular, the focus is on the effect of changing C_a on T_l using a newly proposed model that connects

optimal leaf-gas exchange and leaf heat exchange by using explicit interrelations between g, A, E, T_a, T_l, l_c, and v_w.

To achieve this target model while maintaining tractability, the so-called "reduced order model" of leaf-gas exchange derived elsewhere (Konrad, Katul, Roth-Nebelsick, & Grein, 2017) is coupled to established formulations describing the simultaneous leaf energy and radiation budgets (Jones, 2013; Nobel, 2005). The modelled parameters are g, A, E, and T_l, explored here under light saturation conditions and imposed environmental conditions prescribed in the atmosphere outside the leaf boundary layer (labelled as "free stream variables"). These free stream variables include v_w, C_a, and T_a for different leaf sizes l_c. The model is tested using gas exchange measurements and literature data.

2 | THE MODEL

The target model combines the leaf energy balance with leaf gas exchange for CO_2 and water vapour as well as biochemical demand for CO_2. Hence, the target model parameters are those associated with the aforementioned processes. For tractability, a number of simplifications are necessary in the target model. Steady-state conditions are assumed so that the atmospheric supply and biochemical demand for CO_2 are in balance. Also, the leaf interior is assumed to be saturated so that within the sub-stomatal cavity, the relative humidity of air is 100%. This assumption is reasonable provided leaf water potential does not drop below −5 MPa (Farquhar & Raschke, 1978, but see Cernusak et al., 2018). The leaf interior is also assumed to be in thermal equilibrium with the leaf surface so that the leaf surface temperature can be used to approximate the saturation and actual vapour pressure within the sub-stomatal cavity using the Clausius–Clapeyron equilibrium equation. Minor temperature differences between abaxial and adaxial leaf side can arise (Rockwell, Holbrook, & Stroock, 2014) that can, however, be neglected for the purposes here. Furthermore, mesophyll resistance is not particularly considered in the model though it can be added if known. It is also assumed that the conditions just outside the leaf boundary layer or the free stream are quasi-stationary and spatially uniform so that the main spatial gradients are those associated with processes within the leaf boundary layer. Free convection is not included, which becomes relevant at extremely low wind speeds. The model also considers leaf-level processes in isolation and hence caution must be exercised when extrapolating its conclusions to larger spatial scales. Any physiological differences between sunlit and shaded leaves are assumed to be entirely captured by parameters in the biochemical demand equation for C_3 plants. Perhaps most restrictive is the assumption that $\kappa = C_i/C_a$ is constant and does not change with environmental conditions (e.g., VPD), where C_i is the internal CO_2 concentration. The model does not consider processes at the large scale, such as aerodynamic interrelations between canopies, wind speed, and local topology. Finally, conditions of substantial water and/or salt stress are not included though such conditions do have significant impact on all the aforementioned processes (Perri, Katul, and Molini, 2019).

2.1 | The gas exchange formulation

The gas exchange formulation is centred around the carbon economy of the leaf: The atmospheric supply of CO_2 to the leaf is given by Fick's diffusion law, or its approximate integrated version, as

$$A = g(C_a - C_i). \tag{1}$$

When atmospheric supply is matched to biochemical demand (i.e., when every CO_2 molecule that collides with the leaf surface and enters through the guard cells into the sub-stomatal cavity is eventually assimilated), then A can also be described by the Farquhar photosynthesis model for C_3 plants given as (Farquhar, Von Caemmerer, and Berry, 1980, 2001)

$$A = q\frac{C_i - \Gamma}{C_i + K} - R_d, \tag{2}$$

thus offering another relation between A and C_i at a prescribed C_a. The parameters associated with the photosynthetic model in Equation (2) are as follows: q is carboxylation limited by Rubisco or RuBP regeneration rate, K is a parameter containing Michaelis–Menten constants of carboxylation and oxygenation, Γ is the CO_2 compensation point, and R_d is the mitochondrial respiration rate. The dependence of the biochemical parameters q, Γ, K, and R_d on T_l is based on biochemical considerations derived elsewhere (Bernacchi, Pimentel, and Long, 2003) and are not repeated here. When only a balance between demand and supply for CO_2 is imposed, the outcome of this balance results in one equation with two unknowns: g and C_i. Hence, the gas exchange formulation remains mathematically "unclosed" and requires additional equations. Denoting the ratio of CO_2 concentration within the leaf and the atmosphere as

$$\kappa = \frac{C_i}{C_a}. \tag{3}$$

Equations (3) and (2) can be used to eliminate C_i and A from Equation (1) to obtain an explicit expression for g given as

$$g = \frac{q(\kappa C_a - \Gamma)}{(\kappa C_a + K)(1-\kappa)C_a} - \frac{R_d}{(1-\kappa)C_a}. \tag{4}$$

A number of points can be made about the mathematical character of this expression when noting that κ is a constrained quantity robust to changes in C_a, and to a leading order, may be treated as a constant. Some support for the insensitivity of κ to C_a has been documented in a number of studies reviewed elsewhere (Katul, Ellsworth, and Lai, 2000; Katul, Manzoni, Palmroth, and Oren, 2010). To begin with, increasing C_a while maintaining κ approximately constant means that the "reduction term" that includes R_d (the second term on the right-hand side of (4)) becomes negligible and has minor impact on g except for small C_a. More significant is the first term on the right-hand side of (4) and its dependence on C_a. While the numerator is

linear in C_a, the denominator is quadratic in C_a, meaning that increasing C_a must lead to a reduction in g for high C_a (and conversely for very low C_a). Employing expression (3), the assimilation rate becomes

$$A = q\frac{\kappa C_a - \Gamma}{\kappa C_a + K} - R_d. \tag{5}$$

Different from the g expression in (4), the numerator and denominator of the right-hand side of (5) are both linear in C_a, meaning that leaf photosynthesis (and by extrapolation the capacity of the biosphere to absorb atmospheric CO_2 when maximal leaf area is attained) are expected to "saturate" at $q - R_d$ when C_a is very large. Fick's Law of diffusion for water vapour also leads to

$$E = g\bar{a}(w_l - w_a) = \frac{q(\kappa C_a - \Gamma) - R_d(\kappa C_a + K)}{(\kappa C_a + K)(1-\kappa)C_a}\bar{a}(w_l - w_a), \tag{6}$$

where $\bar{a} := D_{H_2O}/D_{CO_2}$ denotes the ratio of the molecular diffusional coefficients of water vapour and CO_2 in air and w_l is the water vapour concentration within the leaf. The model featured in (1) through (6) assumes that all kinetic parameters as well as w_l depend on T_l and not the commonly available (or projected) T_a. Figure 1a, b, and c illustrates the results from Equations (4), (5) and (6) for g, A and E as functions of C_a and T_l, momentarily assuming isothermal conditions ($T_l = T_a$). The calculations assume that κ is constant determined from isotopic measurements though it can be allowed to vary. To accommodate such variations in κ, an additional equation (and model assumptions) are needed. One common approach to arrive at such an expression is to assume that leaves maximize A subject to some constraints such as water availability per unit leaf area in the rooting zone. Such optimization theories show that κ weakly varies with VPD with a sub-unity exponent and with several schemes predicting approximate scaling relations of the form $\kappa \propto \sqrt{\text{VPD}}$ (Hari, Mäkela, Berninger, and Pohja, 1999; Katul, Palmroth, and Oren, 2009; Katul et al., 2010; Medlyn et al., 2011; Prentice, Dong, Gleason, Maire, and Wright, 2014). This scaling appears to be robust to the precise assumptions made about the constraints imposed on the optimization as discussed elsewhere (Dewar et al., 2018). As expected from such analysis, increasing C_a increases A at all temperatures (in a non-linear manner) though the interplay between C_a and T_a is far more complex for the remaining two variables (g and E). To allow for differences between T_l and T_a, additional expressions are needed to describe the combined leaf energy and radiation balances.

2.2 | The leaf energy exchange equations

To allow for leaf and air temperature differences in the target model, a conventional leaf energy balance formulation (Nobel, 2005; Jones, 2013) is introduced to express T_l in terms of T_a and g. For steady-state conditions, the leaf energy balance equation is given by

$$\begin{aligned}\text{energy into leaf} &= \text{energy out of leaf} \\ &+ [\text{energy consumed by leaf metabolism}].\end{aligned} \tag{7}$$

Since the energy consumed by leaf metabolism is negligible compared to the amounts of energy flowing into and out of the leaf, it is ignored in what follows. Also, it is assumed that leaves have high thermal inertia (or volumetric heat capacity), so that any imbalance between the left hand side and the right hand side in unsteady conditions do not alter T_l appreciably over the time scales considered here (i.e., changes in the environmental conditions external to the leaf). Keeping only the terms that quantify the energy exchange processes leads to (Nobel, 2005)

$$\begin{aligned}a(1+r)S_c\tau_N^{1/\sin\gamma}\sin\gamma + a_{IR}\sigma\left(T_{surr}^4 + T_{sky}^4\right) \\ \approx 2e_{IR}\sigma T_l^4 + \frac{2K_a}{d_{bl}}(T_l - T_a) + 2H_{vap}[w_l(T_l) - w_a]\bar{a}g(T_l).\end{aligned} \tag{8}$$

The terms on the left-hand side quantify the absorption of radiation coming directly from the sun (shortwave radiation), from the closer surroundings (such as other plants) and of diffuse radiation from the sky (longwave radiation). The right-hand side quantifies radiation emitted by the leaf (first term) and heat exchange via conduction and convection (second term) and evaporative cooling by transpiration. Notice that the last term on the right-hand side can be written, due to (6), as $H_{vap}E$, where H_{vap} is the latent heat of vaporization. Table 1 presents the definitions and typical values of the other parameters in Equation (8). The conduction/convection term depends on the thickness d_{bl} of the laminar boundary layer attached to the leaf surface and on the free stream wind velocity v_w as well as the characteristic leaf length l_c. In principle, v_w experiences turbulent fluctuations, and it is often replaced by its time-averaged value. In this case, the turbulent intensity can also play a role in determining d_{bl} because the laminar boundary layer may be intermittently disturbed by the outer turbulent state and may not attain its full steady-state value. However, such effects are usually absorbed in empirical constants of expressions such as the formula of Nobel, 2005 that is suitable for flat surfaces, such as angiosperm leaves and is given by

$$d_{bl} = 4 \times 10^{-3}(\text{m}/\sqrt{\text{s}})\sqrt{\frac{l_c}{v_w}}, \tag{9}$$

(m and s denote the units meter and second, respectively). As expected, d_{bl} increases with increasing l_c and is reduced with increasing v_w. As earlier noted, the leaf internal humidity w_l is close to its saturation value $w_{sat}(T_l)$ that only depends on leaf temperature T_l. In a closed system at thermal equilibrium, the Clausius–Clapeyron equation (Reif, 1974) may be used and it is given as

$$w_l(T_l) \approx w_{sat}(T_l) = \frac{u}{T_l}e^{\left(-\frac{v}{T_l}\right)}, \tag{10}$$

TABLE 1 The model parameters together with their dimensions

Quantity [unit]	Explanation	Value
Physiologic parameters		
A [μmol/m^2/s]	Assimilation rate	Calculated
g [m/s]	Leaf conductance	Calculated
E [mmol/m^2/s]	Transpiration rate	Calculated
C_i [mol/m^3]	Leaf internal CO_2	Calculated
T_l [°C]	Leaf temperature	Calculated
w_l [mol/m^3]	Leaf internal humidity	≈saturated
l_c [mm]	Characteristic leaf length	Varied
κ [–]	κ: = C_i/C_a	0.768
$T_{i,\,c}$ [°C]	Temperature separating the regimes of leaf warming and leaf cooling	Calculated
$T_{i,\,\infty}$ [°C]	Special case of temperature $T_{i,\,c}$ for vanishing transpiration	Calculated
Environmental parameters		
C_a [mol/m^3]	Atmospheric CO_2	Varied
T_a [°C]	Air temperature	Varied
w_a [mol/m^3]	Leaf external humidity	Varied
w_{sat} [mol/m^3]	Saturation value of humidity (cf. expression (10))	Calculated
w_{rel}	Relative atmospheric humidity, $w_{rel} = w_a/w_{sat}$	Varied
v_w [m/s]	Wind velocity	Varied
d_{bl} [mm]	Thickness of boundary layer (cf. expression (9))	Calculated
S_c [J/m^2/s]	Solar constant	1,366
σ [J/m^2/s/K^4]	Stefan-Boltzmann constant	5.67×10^{-8}
K_a [J/m/s/K]	Coefficient of thermal conductivity of air at 20°C	2.55×10^{-2}
H_{vap} [J/mol]	Vapourisation heat of water	44.1×10^3
γ	Angle of sun above horizon	45°
τ_N [–]	Atmospheric transmittance for moderate clear sky at moderate elevation	≈0.7
a [–]	Absorptance of leaf for global radiation	≈0.60
r [–]	Reflectance of the surroundings for global radiation	≈0.20
a_{IR} [–]	Leaf absorptivity for infrared radiation	≈0.96
e_{IR} [–]	Leaf emissivity for infrared radiation	≈0.96
T_{surr} [°C]	Temperature of the surroundings	≈15
T_{sky} [°C]	Radiation temperature of the clear sky	≈ − 20
D_{CO_2} [m^2/s]	Diffusion constant of CO_2 at T = 25°C	1.55×10^{-5}
D_{H_2O} [m^2/s]	Diffusion constant of water vapour at T = 25°C	2.49×10^{-5}
$\bar{a}$	$\bar{a} = D_{H_2O}/D_{CO_2}$	1.6
Biochemical parameters from Quercus petraea		
q [μmol/m^2/s]	Carboxylation limited by Rubisco or RuBP at T = 25°C	58
K [μmol/m^3]	Contains Michaelis–Menten constants	6,926
Γ [μmol/m^3]	CO_2 compensation point	1,584
R_d [μmol/m^2/s]	Mitochondrial respiration rate	1.0

Note: Specific values of parameters designated as "varied" are given in the figure captions.

with $u = 2.035 \times 10^{10}$mol/m^3 and $v = 5{,}306$ (T_l in Kelvin). This equation must be viewed as approximate because the sub-stomatal cavity is not closed to mass exchange (i.e., $E > 0$). However, even for such a system, corrections to the Clausius–Clapeyron equation are small when steady-state conditions are attained. Notice that the radiation and evaporation terms in (8) are always positive, because these two mechanisms only allow the emission of energy from the leaf, whereas the processes of conduction/convection can—depending on the sign of the difference $T_l - T_a$—decrease or increase the leaf's energy content.

Figures 2 and 3 illustrate the various components of the leaf energy balance Equation (8) as they change with T_a: The black line denotes the left-hand side, that is, the radiative energy absorbed by the leaf. The three coloured curves represent the right-hand side, namely emitted radiation (red), conduction/convection processes (green), and evaporation (blue). Their sum equals—for any given T_a—

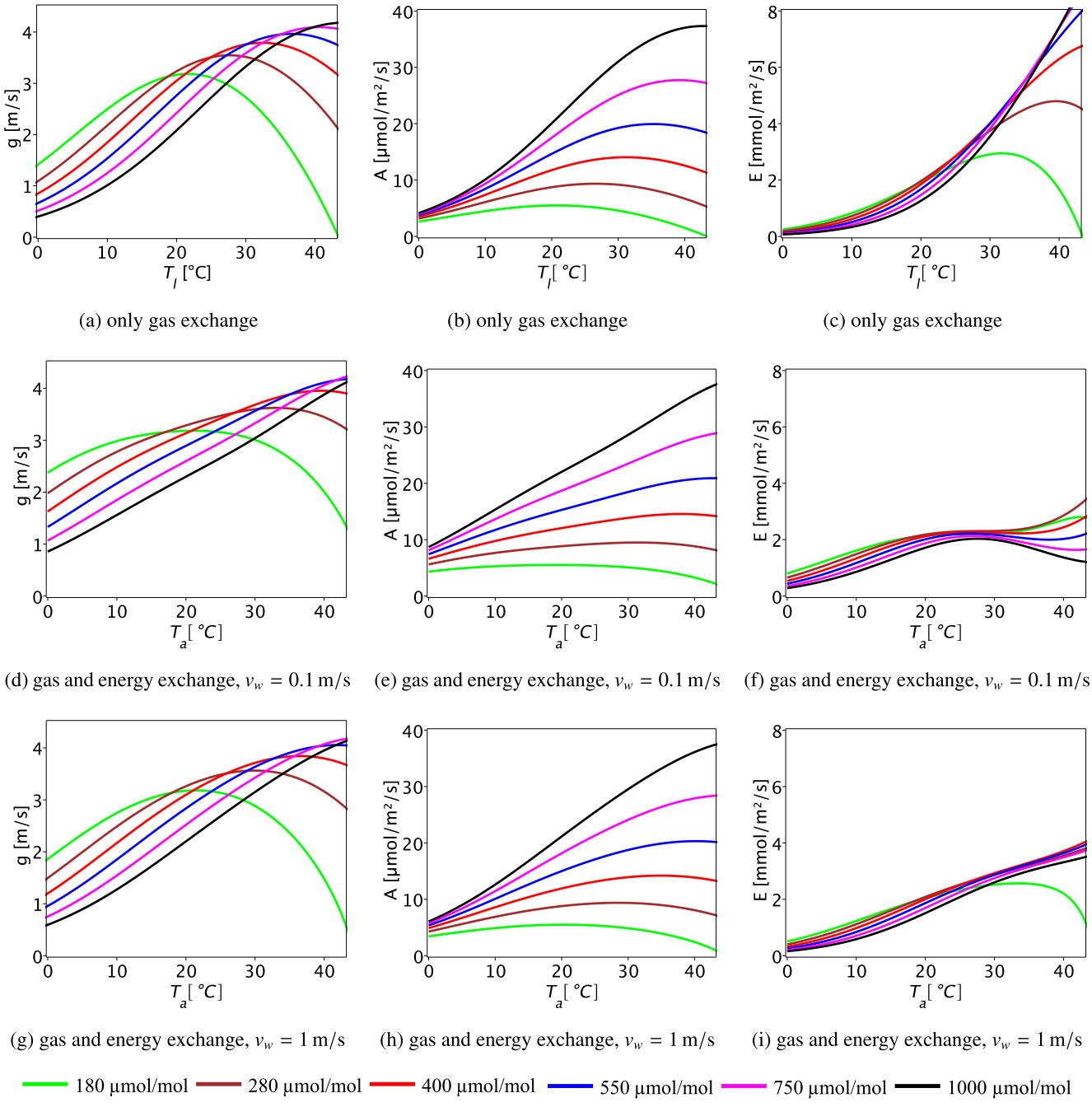

FIGURE 1 Impact of air temperature T_a and atmospheric CO_2 on temperature dependence of leaf conductance g, assimilation rate A, and transpiration rate E. (a–c) Upper row: curves result from the gas exchange equations when ignoring the leaf energy exchange. This assumption is equivalent to setting $T_l = T_a$. Lower two rows: energy exchange between leaf and air, according to relation (8), is taken into account, implying $T_l \neq T_a$. Free stream values: relative humidity $w_{rel} = 0.6$, wind speed $v_w = 0.1$ m/s (subfigures [d–f]), $v_w = 1$ m/s (subfigures [g–i]), characteristic leaf length $l_c = 30$ mm. Other values are as given in Table 1 (biochemical parameters were borrowed from *Quercus petraea*) [Colour figure can be viewed at wileyonlinelibrary.com]

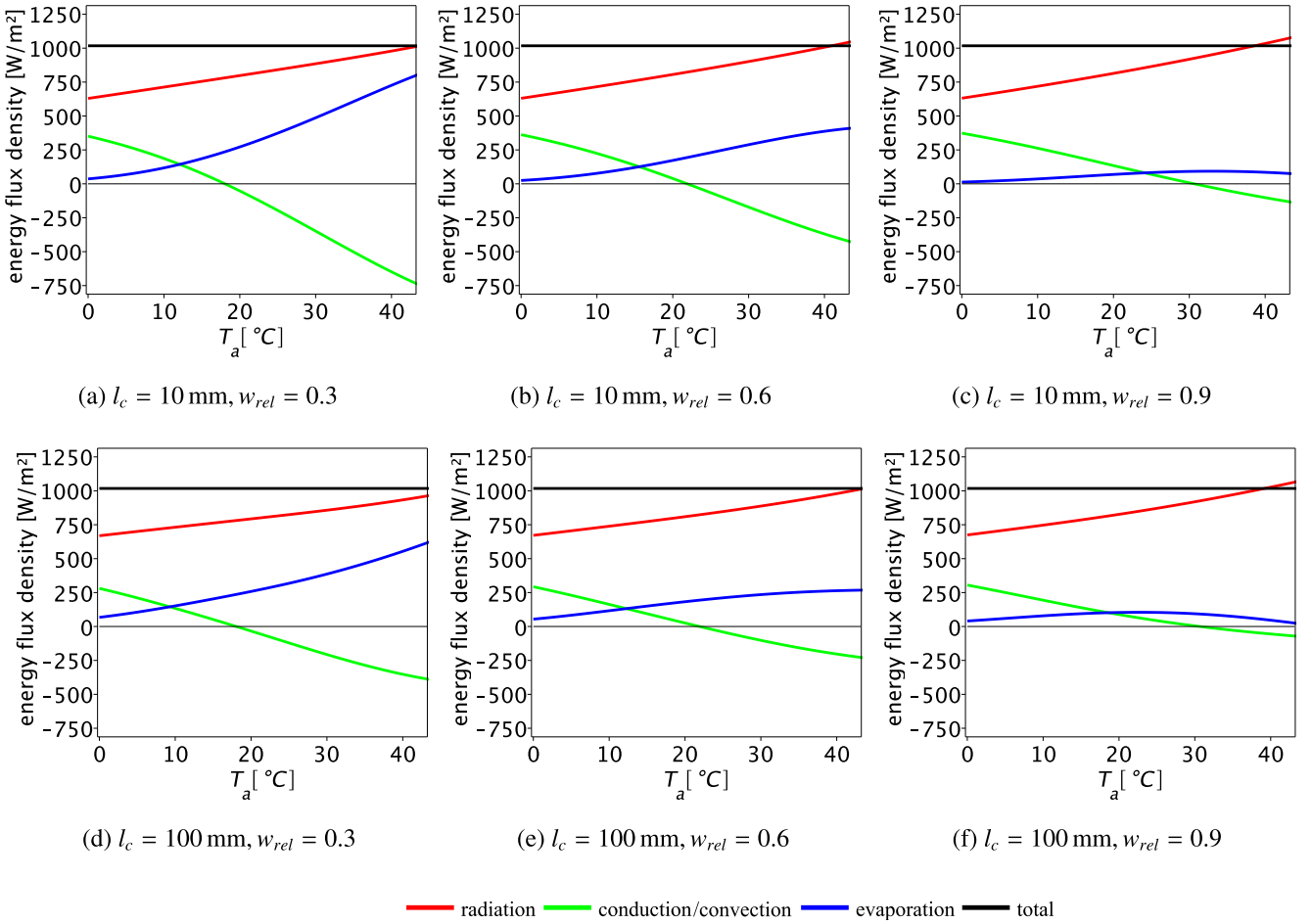

FIGURE 2 The individual components impacting the steady-state leaf energy balance as a function of air temperature T_a and characteristic leaf length l_c. The black lines indicate the total heat absorbed by the leaf, and the coloured lines indicate the mechanisms by which the heat is distributed: radiation (red lines), conduction, and convection (green lines) and evaporation (blue lines). Input values: wind speed v_w = 1 m/s, C_a = 400 μmol/mol. Other input values are as given in Table 1 (biochemical parameters were borrowed from *Quercus petraea*) [Colour figure can be viewed at wileyonlinelibrary.com]

the black line. The conduction/convection is the only term that can be bidirectional and is one reason why results from leaf energy balance calculations can be counter-intuitive on some occasions. Comparison of the sub-figures of Figures 2 and 3 suggests that radiation is almost unaffected by variations of air humidity and leaf size, whereas conduction/convection and evaporation are strongly influenced, which is what one would expect from the physics of this situation.

2.3 | The target model: Combining the leaf gas and energy exchange formulations

If the quantities appearing on the left hand side of Equation (8), the species specific photosynthetic parameters defining the Farquhar biochemical demand model, and the free stream state parameters C_a, v_w, T_a, and w_a (or, alternatively, VPD = $w_l - w_a$) are provided, Equations (4) and (8) (together with (9) and (10)) can be viewed as a system of two algebraic equations for the two unknowns g and T_l.

In principle, the solution procedure is straightforward: Insertion of (4) into (8) (to eliminate g) produces an intricate equation for T_l that admits no closed-form expression. However, the solution simplifies considerably upon the substitution of a canonical form

$$T_l = T_a(1+\xi), \tag{11}$$

followed by a Taylor series expansion with respect to ξ around $\xi = 0$. Since the difference between T_l and T_a is small with respect to T_a (in K), (implying $\xi \ll 1$), it is justified to discard from the expansion higher order terms beyond quadratic (ξ^2). Solving the resulting quadratic equation for ξ and inserting the outcome into (11) yields T_l. Insertion of T_l in expression (4) for g completes the solution process. It is to be noted that $1/g$, the reciprocal of leaf conductance g, combines in series both stomatal and aerodynamic resistances according to

$$\frac{1}{g} = \frac{1}{g_s} + \frac{1}{g_{bl}}. \tag{12}$$

Because $g_{bl} = D_{CO_2}/d_{bl}$, it is possible to use (4) to separate g_s from g. Figure 4 features the resistances $1/g_s$ (solid lines) and $1/g_{bl}$ (dashed lines) that are related to stomatal conductance and boundary layer conductance. According to (12), the sum of related curves equals the

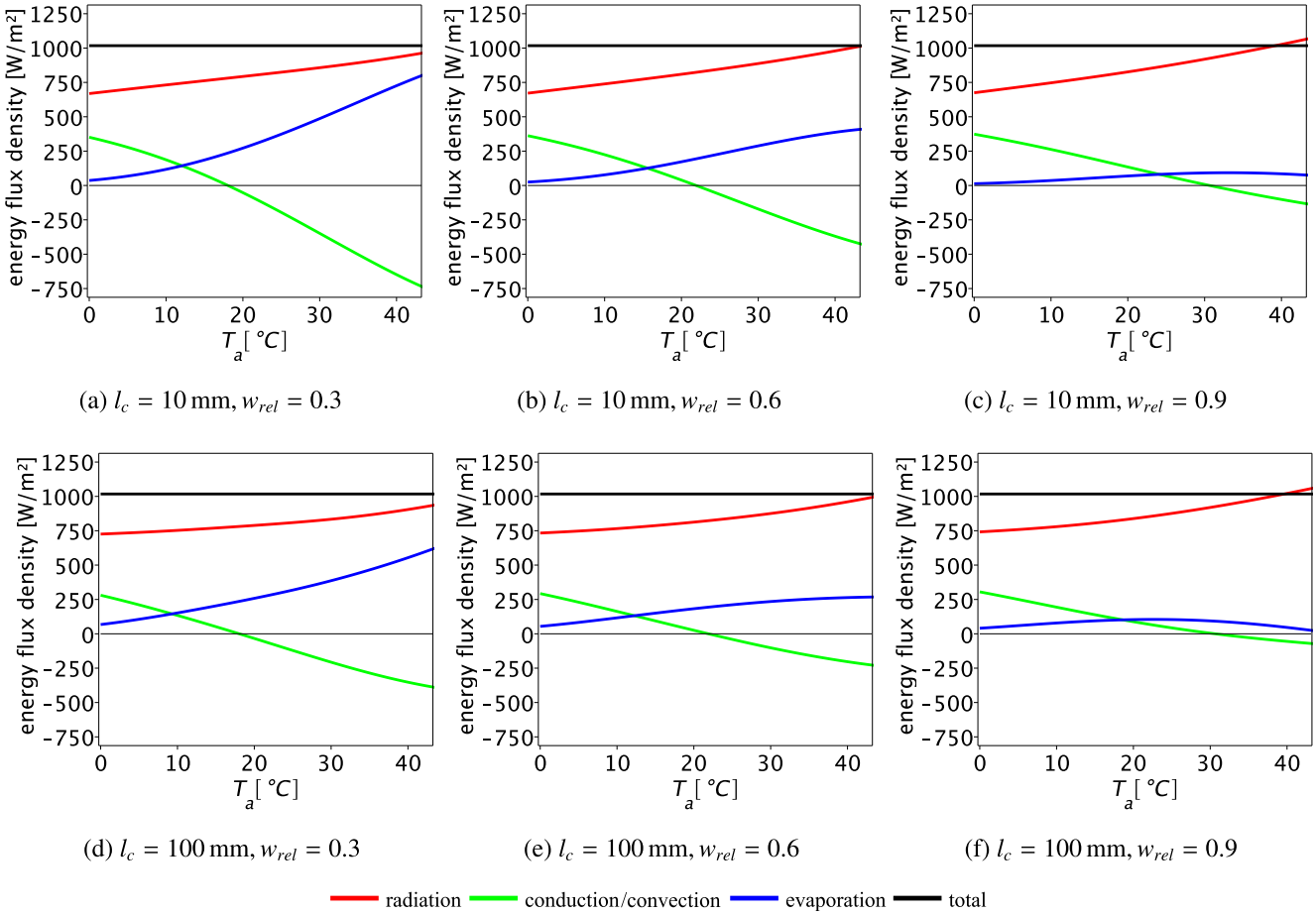

FIGURE 3 The individual components impacting the steady-state leaf energy balance as a function of air temperature T_a and characteristic leaf length l_c. The black lines indicate the total heat absorbed by the leaf, and the coloured lines indicate the mechanisms by which the heat is distributed: radiation (red lines), conduction and convection (green lines) and evaporation (blue lines). Free stream values: wind speed v_w = 0.1 m/s, C_a = 400 μmol/mol. Other input values are as given in Table 1 (biochemical parameters were borrowed from *Quercus petraea*) [Colour figure can be viewed at wileyonlinelibrary.com]

total leaf resistance $1/g$, the reciprocal of leaf conductance. As shown in Figure 4, for small leaves and high wind speeds (Figure 4d), stomatal resistance is much higher than boundary layer resistance; if leaf size increases and wind speed decreases, both resistances become comparable (Figure 4c). The behaviour of the boundary layer resistance is a direct consequence of expression (9) for the thickness of the boundary layer whereas stomatal resistance includes all the radiation, energy, and leaf gas exchange processes.

3 | APPLICATION OF THE MODEL TO LEAF HEATING AND COOLING

The target model is now applied to *Quercus petraea* to illustrate the mechanisms of leaf heating and cooling. This species is chosen because of its wide-spread distribution (and economical value) within Europe, and its well-studied physiological and radiative properties. The *Q. petraea* biochemical parameters used are given in Table 1. Specifically, the effect of complementing the leaf gas exchange equations of Section 2.1 with the energy exchange equations of Section 2.2 is depicted by Figure 1. The upper row of sub-figures follows from the gas exchange equations alone (ignoring leaf energy exchange by setting $T_l = T_a$), the lower row of sub-figures results from coupling both models thereby distinguishing T_l from T_a with all kinetic parameters driven by T_l. If leaf energy exchange is taken into account, the maxima of the curves representing g and A are shifted to higher values of T_a, but the general structure of the family of curves—especially the highly different g- and A-values for identical T_a- but different C_a-values—remains the same. Much more affected by the inclusion of energy exchange is the transpiration rate E that shows (a) a much smaller gradient with respect to T_a and (b) a lesser dependence on C_a.

As already stated, the photosynthetic parameters q, Γ, K, and R_d of the model of Farquhar et al., 1980; see expression (2)) depend on T_l according to the relations of Bernacchi et al. (2003). The interplay of these individual dependencies results in the overall temperature dependence of the assimilation rate A shown in Figure 1b, e, and h that exhibits a maximum of A at some (C_a-dependent) optimum temperature T_{opt}. Obviously, elevated C_a shifts T_{opt} towards higher values. This effect is also observed experimentally as discussed elsewhere (Duursma et al., 2014; Eamus, Duff, and Berryman, 1995; Ghannoum

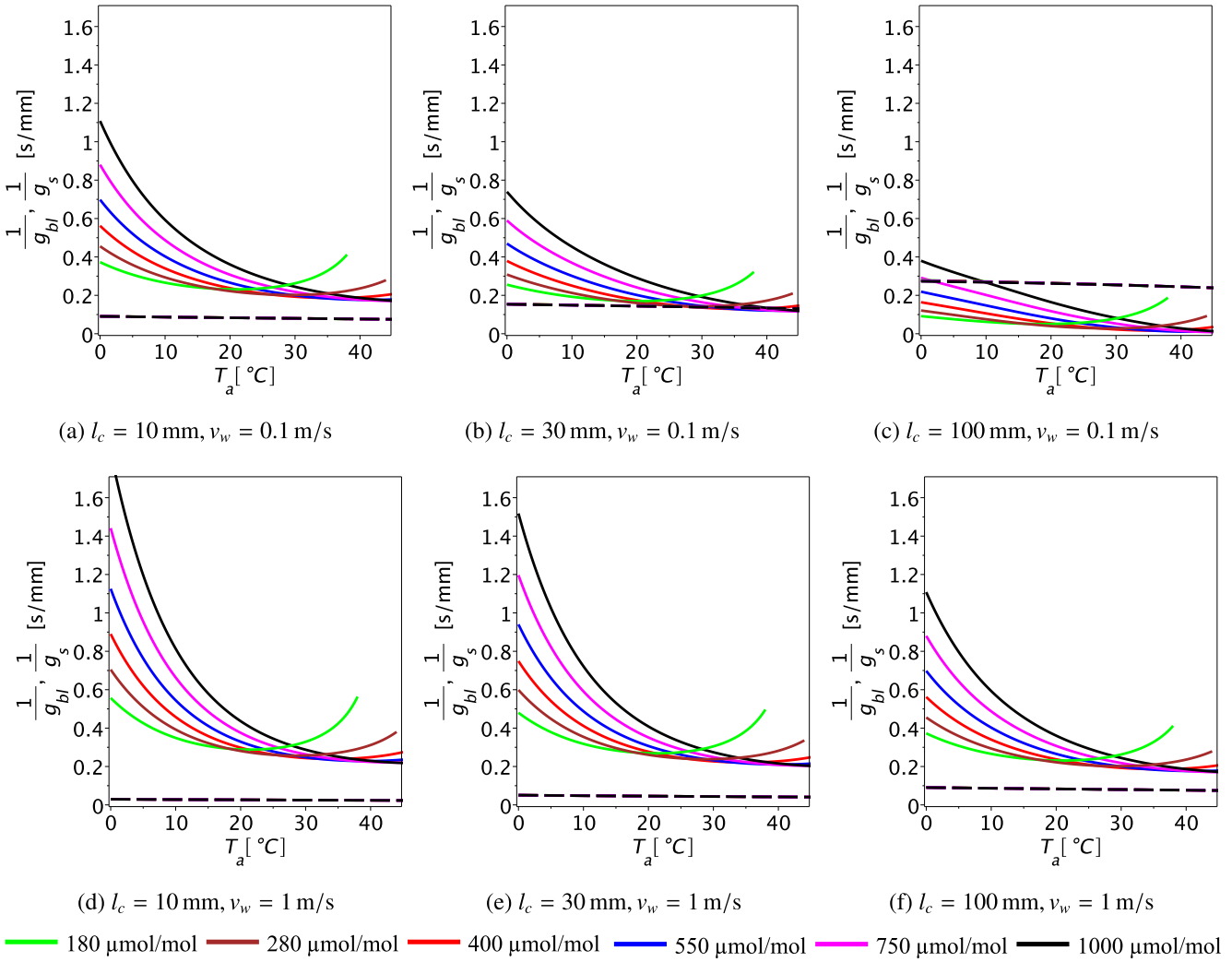

FIGURE 4 Impact of air temperature T_a, atmospheric CO_2, and characteristic leaf length l_c on stomatal resistance $1/g_s$ (solid lines) and boundary layer resistance $1/g_{bl}$ (dashed lines). The sum of these curves sets the total leaf resistance related to leaf conductance and amounts to $1/g = 1/g_{bl} + 1/g_s$. Free stream values: relative humidity $w_{rel} = 0.6$. Other input values are as given in Table 1 (biochemical parameters were borrowed from *Quercus petraea*) [Colour figure can be viewed at wileyonlinelibrary.com]

et al., 2010; Quentin, Crous, Barton, and Ellsworth, 2015; Reef et al., 2016). Notice that the maxima of $g(T_a)$ and $A(T_a)$ are located at the same temperature, T_{opt}. This is not a coincidence, and it directly follows from Equations (1) and (3) that imply

$$g = \frac{A}{(1-\kappa)C_a}. \tag{13}$$

Since it is assumed that κ = const. and since C_a does not depend on local leaf or air temperature here, g inherits its temperature dependence from A described above and depicted in Figure 1.

3.1 | Mechanisms of leaf heating and cooling

Figures 5 and 6 are now used as a starting point to unravel the interplay of the various contributions to leaf heating and cooling. The coloured curves feature the dependency of leaf temperature on air temperature for different leaf sizes and several values of free stream air relative humidity. The diagonal thin black lines indicate equality of leaf and air temperature, that is, $T_l = T_a$. Thus, segments of the coloured curves located above the thin black lines indicate leaf heating, coloured segments below these lines indicate leaf cooling. The dashed black lines result if evaporation is inhibited in (8) by setting $g = 0$.

The coloured lines in Figures 5 and 6 are related to different atmospheric C_a levels. They originate when stomata are open and transpiration, causing evaporative cooling, contributes to the energy exchange between leaf and air. That is, the transpiring leaves make use of all three energy exchange mechanisms to regulate leaf temperature. Since the mechanisms of conduction and convection can transport heat into and away from the leaf, they can cool *or* heat the leaf depending on the sign of $T_l - T_a$. Evaporation, which is based on heat consuming vaporization, in contrast, can transport heat only away from the leaf, that is, cooling it. Figures 5 and 6 suggest that evaporative cooling can have a considerable impact on the temperature $T_{i,c}(C_a)$, which is defined by the intersection of the coloured lines and

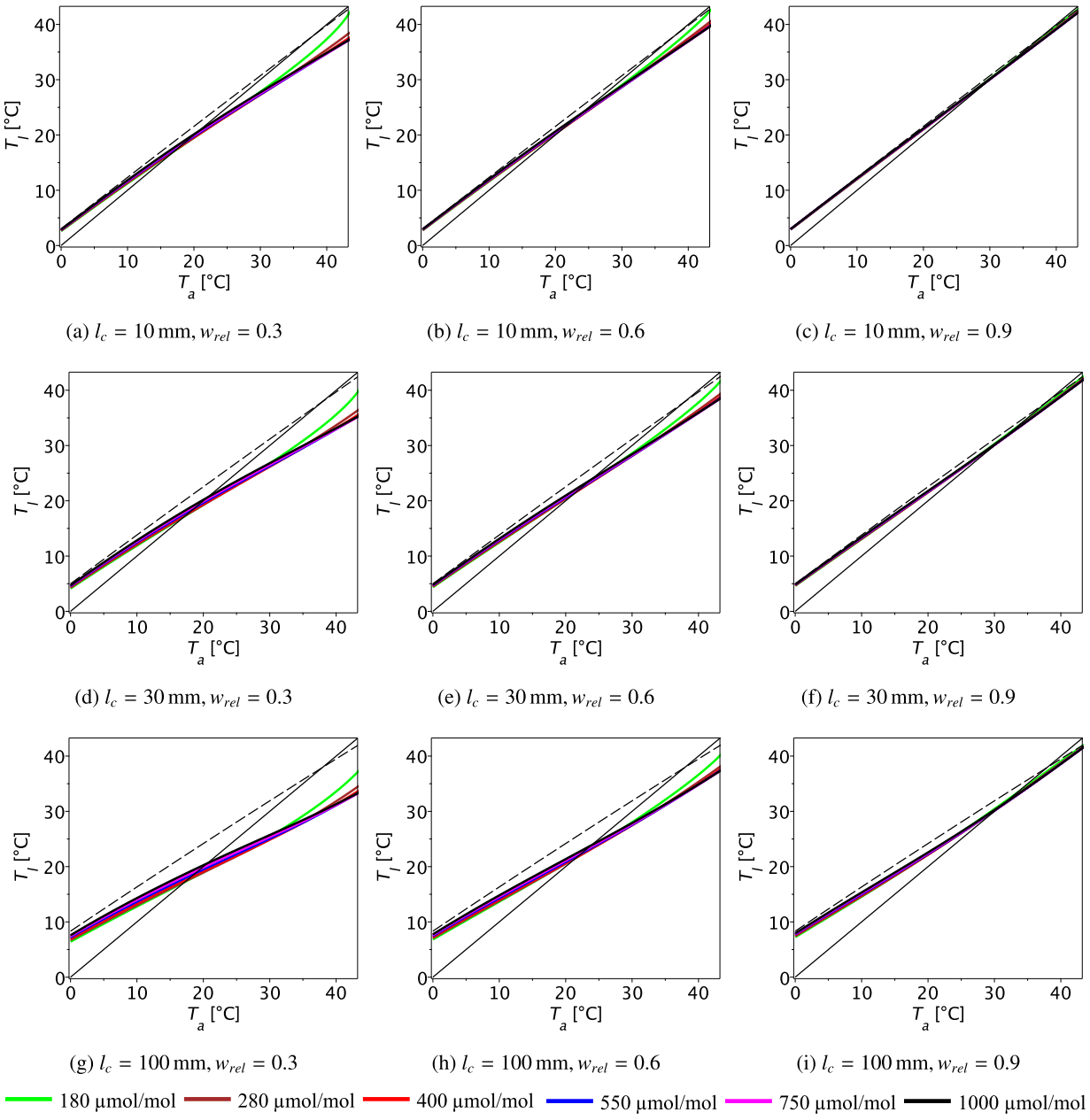

FIGURE 5 Impact of air temperature T_a, atmospheric CO_2, air humidity w_{rel} and characteristic leaf length l_c on leaf temperature T_l. The diagonal thin black lines indicate equality of leaf and air temperature, that is, $T_l = T_a$. Thus, segments of the coloured curves located above the thin black lines indicate leaf heating, and coloured segments below this line indicate leaf cooling. The dashed black lines result if evaporation is inhibited in (8) by setting $g = 0$. The free stream values: wind speed v_w = 1 m/s. Other input values are as given in Table 1 (biochemical parameters were borrowed from *Quercus petraea*) [Colour figure can be viewed at wileyonlinelibrary.com]

the thin black lines, separating the regimes of leaf warming and leaf cooling: If, for instance, C_a is in the range 180 μmol/mol…1,000 μmol/mol and characteristic leaf length and humidity have the values l_c = 30 mm and w_{rel} = 0.6, the related $T_{i,\,c}$-values are in the range 21.6°C…23.9°C. This is about 15 K lower than $T_{i,\,\infty} \approx 37.9^{\circ}$C, the equivalent of $T_{i,\,c}$ for the case of vanishing transpiration derived from (4) for $C_a \to \infty$ (explaining the nomenclature). This case is illustrated by Figures 5e and 6e.

Inspection of Figures 5 and 6 also reveals how $T_{i,\,c}$ depends on air humidity, leaf size, and wind speed:

1. The horizontal sequences a–c, d–f, and g–i in Figures 5 and 6 show that $T_{i,\,c}$ reacts sensitively to increasing air humidity: If w_{rel} is increased from the value 0.3 to 0.9, $T_{i,\,c}$ moves from about 22°C to 30.6°C…32.9°C (for l_c = 30 mm). The reason is obvious: Increasing w_{rel} lowers VPD that impedes transpiration and evaporative cooling.
2. Increasing leaf size l_c (vertical sequences a–g, b–h, and c–i in Figures 5 and 6) does not change the temperature $T_{i,c}$. However, the amount of both leaf warming and cooling increases with l_c for a given air temperature T_a. In Figures 5 and 6, this is clearly visible at the points where both the coloured lines

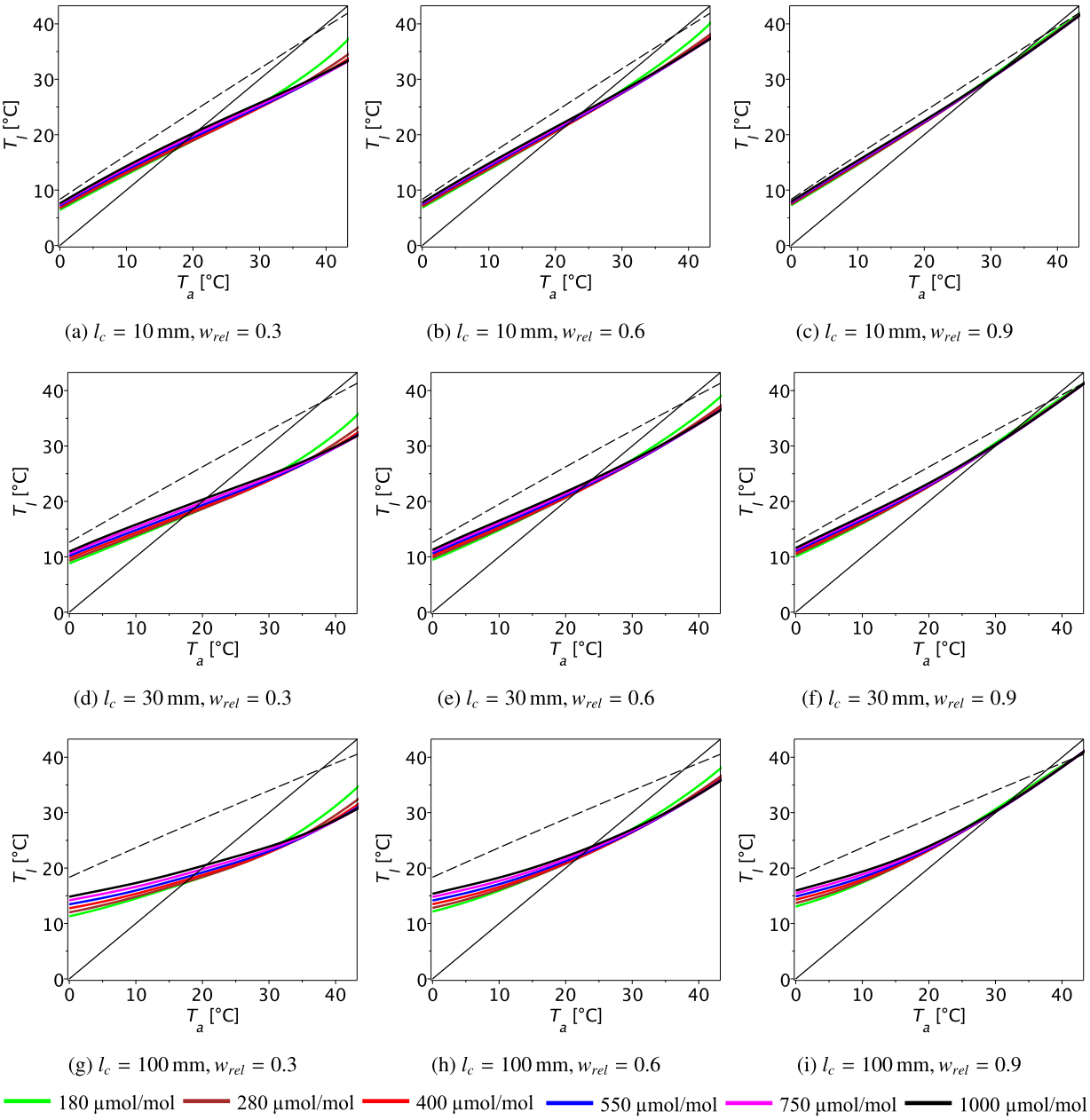

FIGURE 6 Impact of air temperature T_a, atmospheric CO_2, air humidity w_{rel}, and characteristic leaf length l_c on leaf temperature T_l. The diagonal thin black lines indicate equality of leaf and air temperature, that is, $T_l = T_a$. Thus, segments of the coloured curves located above the thin black lines indicate leaf heating, and coloured segments below this line indicate leaf cooling. The dashed black lines result if evaporation is inhibited in (8) by setting $g = 0$. Free stream values: wind speed $v_w = 0.1$ m/s. Other input values are as given in Table 1 (biochemical parameters were borrowed from *Quercus petraea*) [Colour figure can be viewed at wileyonlinelibrary.com]

and the dashed black line (representing the special case $g = 0$ of vanishing transpiration) intersect the T_l-axis.

3. Comparison of Figures 5 and 6 shows that a reduction of wind speed does not change the temperature $T_{i,\,c}$ that separates the regimes of leaf warming and leaf cooling. It enhances, however, both leaf warming and cooling.

The main results of this section are not limited to *Q. petraea*. In the Appendix, we outline how they can be derived from the species-independent model equations of Section 2.

3.2 | Effect of atmospheric CO_2 on leaf temperature

In Figures 5 and 6, the curves related to different C_a-values lie almost on top of one another (with the exception of the green curve, related to subambient C_a, which deviates somewhat from the general trend), indicating that the impact of C_a on T_l is nearly irrelevant. This can be understood from the structure of Equation (8). It depends on C_a solely via the term g (by relation (4)), whereas T_l appears in several terms of which the emission term (containing T_l^4) and the expression $w_l(T_l)$

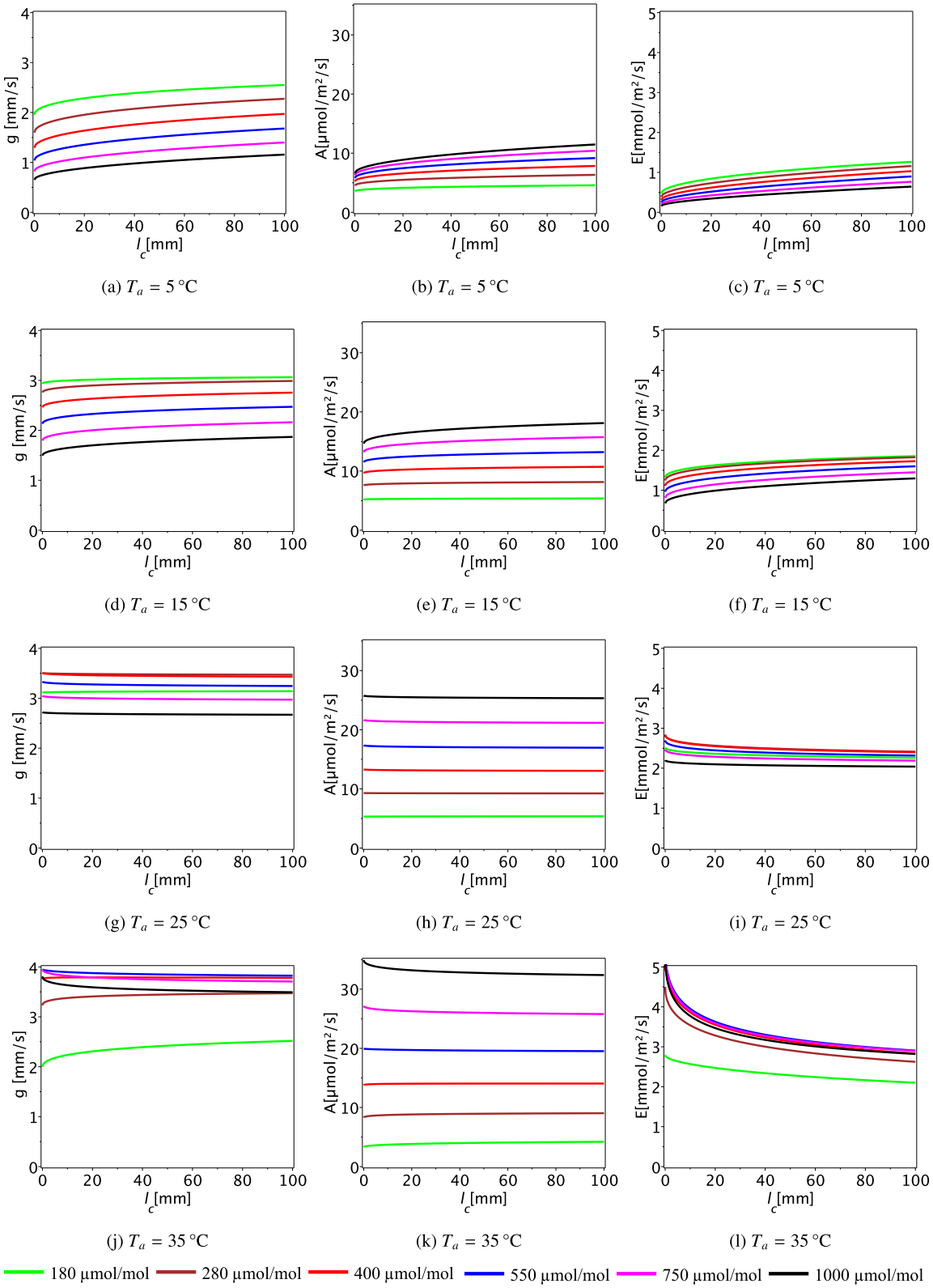

FIGURE 7 Leaf conductance *g* (left column), assimilation rate *A* (centre column), and transpiration rate *E* (right column) as a function of characteristic leaf length l_c for different values of air temperature T_a = (5°C, 15°C, 25°C, 35°C; from top row to bottom row). Wind velocity is v_w = 1 m/s, relative atmospheric humidity is w_{rel} = 0.6. Other input values are as given in Table 1 (biochemical parameters were borrowed from *Quercus petraea*) [Colour figure can be viewed at wileyonlinelibrary.com]

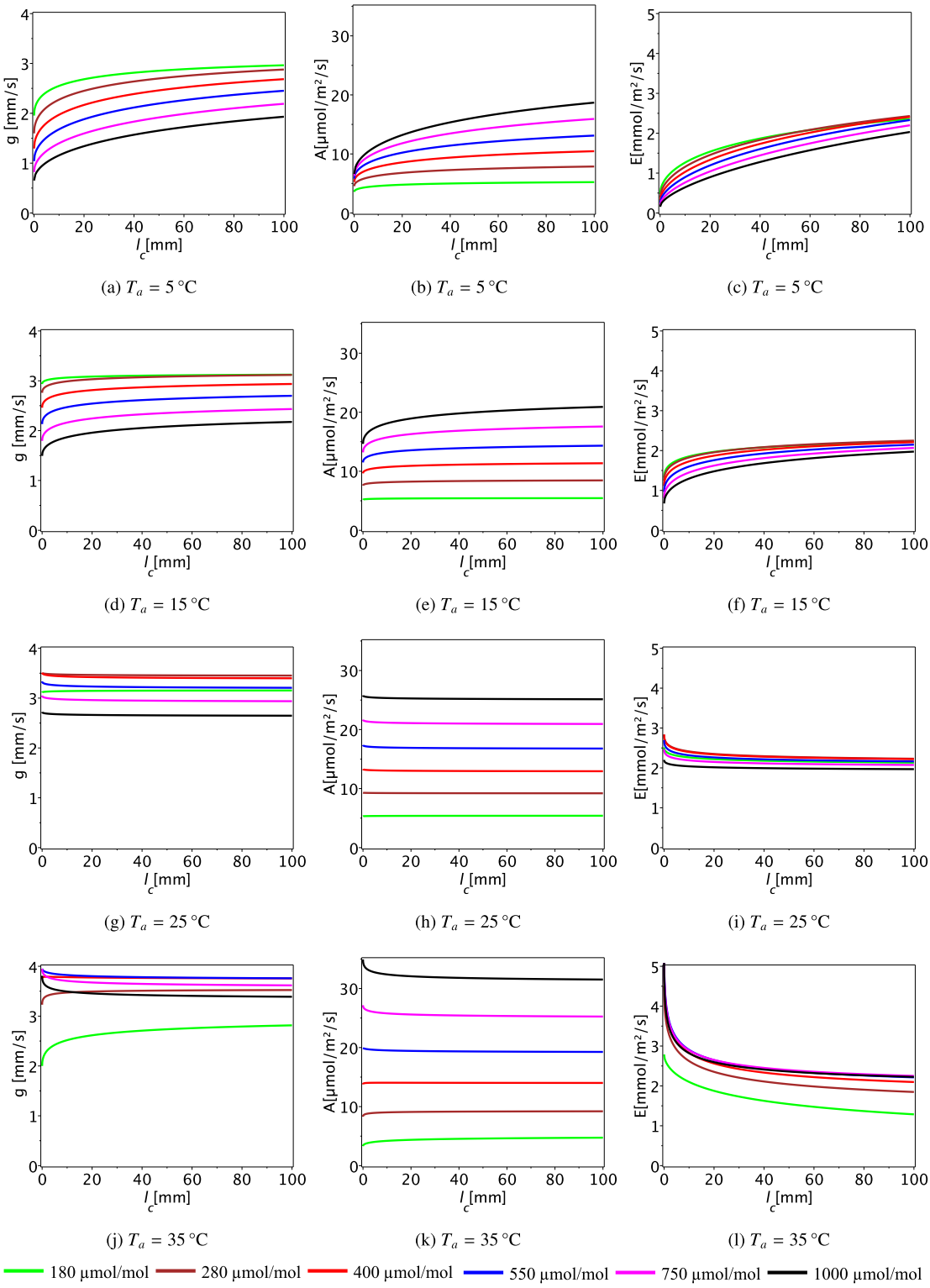

FIGURE 8 Leaf conductance g (left column), assimilation rate A (centre column), and transpiration rate E (right column) as a function of characteristic leaf length l_c for different values of air temperature T_a = (5°C, 15°C, 25°C, 35°C) (from top row to bottom row). Wind velocity is v_w = 0.1 m/s, relative atmospheric humidity is w_{rel} = 0.6. Other input values are as given in Table 1 (biochemical parameters were borrowed from *Quercus petraea*) [Colour figure can be viewed at wileyonlinelibrary.com]

(containing an exponential involving T_l, according to the Clausius-Clapeyron Equation (10)) are especially notable: The fourth power and the exponential effectuate that even large variations in C_a can be balanced by small variations in T_l, provided that all other variables are kept constant and Equation (8) is to be valid.

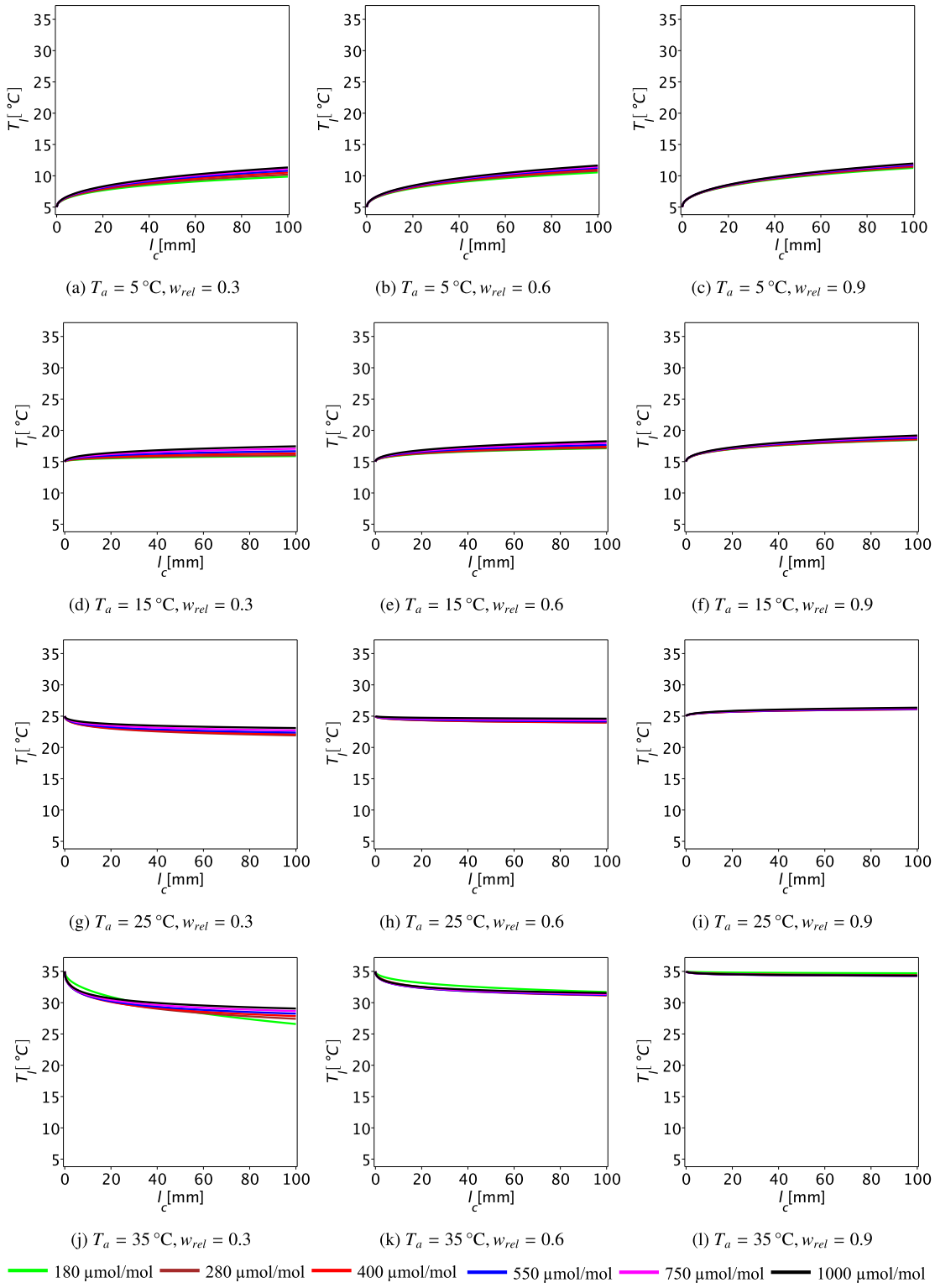

FIGURE 9 Leaf temperature T_l as function of characteristic leaf length l_c for various combinations of air temperature T_a = (5°C, 15°C, 25°C, 35°C) and relative atmospheric humidity w_{rel} = (0.3, 0.6, and 0.9). Wind velocity is v_w = 1 m/s. Other input values are as given in Table 1 (biochemical parameters were borrowed from *Quercus petraea*) [Colour figure can be viewed at wileyonlinelibrary.com]

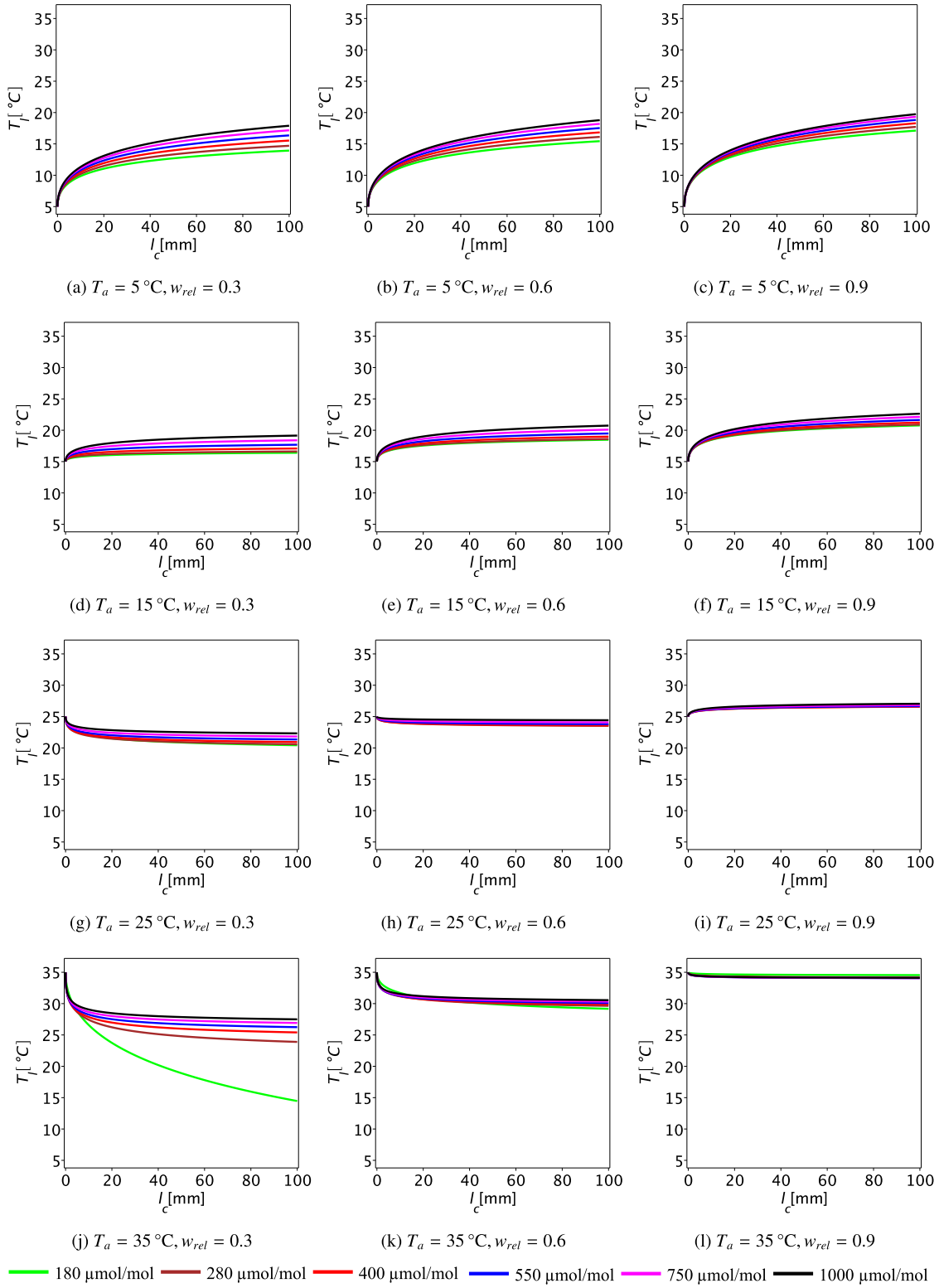

FIGURE 10 Leaf temperature T_l as function of characteristic leaf length l_c for various combinations of air temperature T_a = (5°C, 15°C, 25°C, 35°C) and relative atmospheric humidity w_{rel} = (0.3, 0.6, and 0.9). Wind velocity is v_w = 0.1 m/s. Other input values are as given in Table 1 (biochemical parameters were borrowed from *Quercus petraea*) [Colour figure can be viewed at wileyonlinelibrary.com]

3.3 | Effect of leaf size and wind speed on assimilation rate, transpiration rate, and leaf temperature

Figures 7–10 illustrate the impact of l_c on leaf conductance, assimilation rate, transpiration rate, and leaf temperature if free stream wind speed is varied. All curves share a common feature: Their slopes are steepest for small l_c and decrease smoothly with increasing l_c, such that the curves flatten out more and more. The reason for this behaviour is the way in which l_c enters Equation (8): l_c acts on the conduction/convection term in Equation (8) through the boundary layer thickness that is related to leaf size by $d_{bl} \propto \sqrt{l_c}$, according to (9). This square root dependence explains, at least partly, that size changes in large leaves have much less impact on the dependent variables than size changes in small leaves. Although there is no clear-cut threshold separating both regimes, a value of roughly $l_c \approx 30$ mm seems to be reasonable for which further increases in l_c have minor impacts on g, A, and E.

The most interesting feature of leaf size is its interaction with air humidity and air temperature: Leaves may experience heating (for $T_a \lesssim 20^\circ$C) or cooling (for $T_a \gtrsim 20^\circ$C) depending on T_a. Both effects are much more pronounced for small leaves than for large leaves. Warming occurs also for high humidities (i.e., small VPD), but cooling is in this case very limited due to low transpiration. Ecologically, this temperature compensatory feature makes sense: the warming is beneficial for assimilation, the cooling reduces the hazard of overheating.

Incidentally, Figures 9 and 10 corroborate the nearly negligible dependence of leaf temperature on atmospheric CO_2 already encountered for a fixed leaf size in Figures 5 and 6 for arbitrary values of l_c.

4 | DISCUSSION

There is persistent interest in the ecological role of leaf size and shape, and the selective pressures that underlie the evolution of leaf architecture (Givnish, 1987; Givnish and Vermeij, 1976; Leigh, Sevanto, Close, and Nicotra, 2017; Nicotra et al., 2011; Niinemets et al., 2007; Peppe et al., 2011). While possible functional aspects of leaf size and shape are broad, comprising, for example, self-shading or herbivory (Brown, Lawton, and Grubb, 1991; Falster and Westoby, 2003; Givnish, 1984), it is physically inevitable that the potential thickness of the boundary layer is dictated by them, with consequences for leaf temperature T_l and transpiration rate E.

The model results reported here corroborate various observations and findings on leaf temperature under various environmental conditions (Michaletz et al., 2015; Gates, Hiesey, Milner, and Nobs, 1964; Linacre, 1967; Helliker and Richter, 2008; Pincebourde and Woods, 2012). The proposed model extends these approaches by combining leaf-gas exchange (Section 2.1) with leaf energy balance (Section 2.2), allowing reconstruction and prediction of leaf cooling and heating in environments of different atmospheric CO_2 concentrations.

Whereas the results of this study support the ecological relevance of the characteristic leaf size l_c, no evidence could be found that C_a exerts a selective pressure on l_c via g_s and evaporative cooling, at least on the time scales analysed here. A decrease in g in response to rising C_a has been observed and is predicted by Equation (4) under conditions already discussed. This decrease in g has prompted anticipations that leaf temperatures would increase under elevated C_a as a consequence of reduced evaporative cooling (Beerling and Berner, 2005; Paschalis, Katul, Fatichi, Palmroth, and Way, 2017; Voelker et al., 2016). Figures 5 and 6, however, show that leaf temperature is more robust against variations in atmospheric CO_2 concentration than against variations in leaf size and atmospheric humidity.

As illustrated by the model results, a combination of physical and physiological mechanisms counteracts C_a-induced decrease of evaporative cooling, particularly under conditions of high air temperature. These are highlighted and discussed below.

1. Physiologically, photosynthesis is stimulated strongest when T_l is close to T_{opt} where assimilation rate A and—in view of relation (13)—leaf conductance g are maximal. Figure 1 illustrates that T_{opt} is displaced to higher values when C_a increases. Thus, rising C_a accompanied by increasing T_l ($< T_{opt}$) should promote increasing A and should lead to increased stomatal opening. The increased stomatal opening leads to increased evaporative cooling, and particularly so for high C_a, provided κ is kept constant. Higher g for both elevated C_a and T_a, compared to ambient T_a is actually supported by various experiments (Wang, Heckathorn, Wang, and Philpott, 2012). Slightly higher E under elevated C_a and high VPD has also been reported by whole-tree-flux measurements (Duursma et al., 2014).
2. Physically, leaf heating increases the saturation vapour pressure of the leaf internal air. When assuming that air humidity outside the leaf (i.e., the free stream value) is not changing drastically (even under elevated C_a), it is expected that evaporation and thus evaporative cooling will be enhanced (Campbell and Norman, 1998).

When assessing the anticipated decrease in g as a response to rising C_a, one should keep in mind that the decisive quantity representing evaporative cooling in Equation (8) is transpiration E. This quantity is formed from the product of g and $(w_l(T_l) - w_a)$, according to (6). Comparison of Figure 1d and f shows that E responds to variations in C_a and T_l mildly, in contrast to g that exhibits a much more pronounced dependence on both C_a and T_l. The reason for that is the factor $(w_l(T_l) - w_a)$: (a) Its steep, positive slope with respect to T_l attenuates the negative slope exhibited by g for $T_l < T_{opt}$ (as illustrated by Figure 1f,i) and (b) it dominates the product $E = \bar{a}(w_l - w_a)g$ with respect to temperature and "squeezes" the separated curves of Figures 1d,g into the compact bands of Figures 1f,i. This closeness of the curves related to different C_a-values implies that rising C_a will not cause a tremendous increase of leaf temperature, if any.

As pointed out in Section 3.1, evaporative cooling is not the only mechanism that provides leaf cooling. The combination of radiation emission and heat conductance/convection contributes also to a leaf cooling effect. The work here shows that this cooling effect comes

into operation for $T_a > T_{i,\infty}$ ($T_{i,\infty}$ has been defined in 3.1: It measures the expected leaf temperature in the absence of evaporative cooling). As typical value for $T_{i,\infty}$, we found above $T_{i,\infty} \approx 37.9^{\circ}$C. Thus, this mechanism intensifies leaf cooling if temperatures have already risen to values that are dangerous for vital leaf functions.

The combination of physical and physiological mechanisms leads to the circumstance that values of T_l appear to be weakly affected by elevated C_a, regardless of leaf size (see Figures 9 and 10). The anticipated phenomenon of leaves heating up under elevated C_a may therefore be largely non-existent.

These results are in contrast to expectations that periods of elevated C_a generate necessarily rising leaf temperatures (Cernusak et al., 2013; Paschalis et al., 2017) as well as for the past (Haworth et al., 2014; Lee, Upchurch, Murchie, and Lomax, 2015; McElwain, Beerling, and Woodward, 1999). For the past, C_a is usually expected to represent a crucial element for the evolution of leaf shape and size under conditions of high C_a levels (Beerling and Royer, 2011; Lee et al., 2015; McElwain et al., 1999). Atmospheric CO_2 increased and decreased repeatedly during land plant evolution, with levels often close to or even higher than 1,000 ppm (Anagnostou et al., 2016; Beerling and Royer, 2011; Franks et al., 2014; Montañez et al., 2007; Steinthorsdottir and Vajda, 2015). Under such conditions, both smaller leaf size and dissected leaves were suggested as appropriate strategies to avoid excessive leaf temperatures under periods of high C_a (Haworth et al., 2014; Lee et al., 2015; McElwain et al., 1999). According to the results of the present study, elevated C_a does not have the potential to act upon leaf evolution via T_l. This also means that palaeoclimate proxy approaches that include leaf size, such as CLAMP, are not affected by C_a. During periods of supposedly high CO_2, large and entire leaves did in fact not disappear. For example, angiosperm leaf size even increased from the early to the late Palaeocene-Eocene Thermal Maximum, a period of both high C_a and extreme warmth (Wing et al., 2005).

Leaf warming by high l_c is potentially highest under low air temperature T_a, with further enhancement by simultaneously high w_{rel} (see upper two rows of Figures 9 and 10). Large leaves may thus be particularly beneficial in cooler climate zones during the morning hours by stimulating assimilation rate A, as was already suggested by Okajima, Taneda, Noguchi, and Terashima (2012), and in warm and hot climate zones during the afternoon hours by promoting leaf cooling to avoid leaf damage. These functional aspects emphasize the need for knowing leaf temperature when evaluating gas exchange under different environmental conditions (Michaletz et al., 2015).

5 | SUMMARY AND CONCLUSION

The presented model, based on leaf gas exchange and on leaf energy exchange, allows the examination of the inter-dependencies between leaf properties (leaf size and temperature), physiological parameters (leaf conductance, assimilation and transpiration rate) and local environmental variables (air temperature, air humidity, atmospheric CO_2, wind speed, solar and environmental irradiation) in a systematic way. The relations between leaf temperature, atmospheric CO_2 and leaf size provided by the model here imply the following: Leaf temperature depends on leaf size, but is almost independent of atmospheric CO_2 despite reductions in leaf conductance with increased atmospheric CO_2.

CONFLICT OF INTEREST

All authors declare no conflict of interest.

ACKNOWLEDGEMENTS

This manuscript is the extended version of a talk given at the Special Session *Cenozoic plant diversity: Gradients in time and space and their impact on early humans* (ROCEEH/NECLIME) of the EPPC 2018 in Dublin. The authors would like to thank the organizers of this NECLIME session (Angela A. Bruch, Alexandra-Jane Henrot, Louis François, Natalia Rudaya, and Torsten Utescher) for the invitation to contribute to this Special Issue. This study was supported by a grant of the Volkswagen Foundation to A. R. N. within the programme "Research in Museums" (Refs. 87139, 87160, 87160-1). The authors would also like to thank the reviewers for their constructive comments.

ORCID

Wilfried Konrad https://orcid.org/0000-0002-8686-7865

REFERENCES

Ainsworth, E. A., & Rogers, A. (2007). The response of photosynthesis and stomatal conductance to rising [CO_2]: Mechanisms and environmental interactions. *Plant, Cell and Environment*, *30*, 258–270.

Anagnostou, E., John, E. H., Edgar, K. M., Foster, G. L., Ridgwell, A., Inglis, G. N., … Pearson, P. N. (2016). Changing atmospheric CO_2 concentration was the primary driver of early Cenozoic climate. *Nature*, *533*, 380–384.

Beerling, D., Osborne, C., & Chaloner, W. (2001). Evolution of leaf-form in land plants linked to atmospheric CO_2 decline in the late Palaeozoic era. *Nature*, *410*, 352–354.

Beerling, D., & Royer, D. (2011). Convergent Cenozoic CO_2 history. *Nature Geoscience*, *4*, 418–420.

Beerling, D. J., & Berner, R. A. (2005). Feedbacks and the coevolution of plants and atmospheric CO_2. *Proceedings of the National Academy of Sciences of the United States of America*, *102*, 1302–1305.

Bernacchi, C. J., Pimentel, C., & Long, S. P. (2003). In vivo temperature response functions of parameters required to model RuBP-limited photosynthesis. *Plant, Cell and Environment*, *26*, 1419–1430.

Brown, V., Lawton, J., & Grubb, P. (1991). Herbivory and the evolution of leaf size and shape [and discussion]. *Philosophical Transactions of the Royal Society of London B: Biological Sciences*, *333*, 265–272.

Campbell, G., & Norman, J. (1998). *An introduction to environmental biophysics*. New York, USA: Springer-Verlag.

Cernusak, L. A., Ubierna, N., Jenkins, M. W., Garrity, S. R., Rahn, T., Powers, H. H., … Farquhar, G. D. (2018). Unsaturation of vapour pressure inside leaves of two conifer species. *Scientific Reports*, *8*, 7667.

Cernusak, L. A., Winter, K., Dalling, J. W., Holtum, J. A. M., Jaramillo, C., Körner, C., … Wright, S. J. (2013). Tropical forest responses to increasing atmospheric CO_2: Current knowledge and opportunities for future research. *Functional Plant Biology*, *40*, 531–551.

De Boeck, H. J., Van De Velde, H., De Groote, T., & Nijs, I. (2016). Ideas and perspectives: Heat stress: More than hot air. *Biogeosciences*, *13*, 5821–5825.

De Boer, H., Lammertsma, E., Wagner-Cremer, F., Dilcher, D., Wassen, M., & Dekker, S. (2011). Climate forcing due to optimization of maximal leaf conductance in subtropical vegetation under rising CO_2. *Proceedings of the National Academy of Sciences of the United States of America*, *108*, 4041–4046.

Dewar, R., Mauranen, A., Mäkelä, A., Hölttä, T., Medlyn, B., & Vesala, T. (2018). New insights into the covariation of stomatal, mesophyll and hydraulic conductances from optimization models incorporating non-stomatal limitations to photosynthesis. *New Phytologist*, *217*, 571–585.

Doughty, C. E., & Goulden, M. L. (2008). Are tropical forests near a high temperature threshold? *Journal of Geophysical Research: Biogeosciences*, *113*, G00B07.

Duursma, R. A., Barton, C. V. M., Lin, Y.-S., Medlyn, B. E., Eamus, D., Tissue, D. T., … McMurtrie, R. E. (2014). The peaked response of transpiration rate to vapour pressure deficit in field conditions can be explained by the temperature optimum of photosynthesis. *Agricultural and Forest Meteorology*, *189–190*, 2–10.

Eamus, D., Duff, G., & Berryman, C. (1995). Photosynthetic responses to temperature, light flux-density, CO_2 concentration and vapour pressure deficit in eucalyptus tetrodonta grown under co_2 enrichment. *Environmental Pollution*, *90*, 41–49.

Falster, D. S., & Westoby, M. (2003). Leaf size and angle vary widely across species: What consequences for light interception? *New Phytologist*, *158*, 509–525.

Farquhar, G., Von Caemmerer, S., & Berry, J. (1980). A biochemical model of photosynthetic CO_2 assimilation in leaves of C_3 species. *Planta*, *149*, 78–90.

Farquhar, G., Von Caemmerer, S., & Berry, J. (2001). Models of photosynthesis. *Plant Physiology*, *125*, 42–45.

Farquhar, G. D., & Raschke, K. (1978). On the resistance to transpiration of the sites of evaporation within the leaf. *Plant Physiology*, *61*, 1000–1005.

Franks, P. J., Adams, M. A., Amthor, J. S., Barbour, M. M., Berry, J. A., Ellsworth, D. S., … von Caemmerer, S. (2013). Sensitivity of plants to changing atmospheric CO_2 concentration: From the geological past to the next century. *New Phytologist*, *197*, 1077–1094.

Franks, P. J., Royer, D. L., Beerling, D. J., Van de Water, P. K., Cantrill, D. J., Barbour, M. M., & Berry, J. A. (2014). New constraints on atmospheric CO_2 concentration for the Phanerozoic. *Geophysical Research Letters*, *41*, 4685–4694.

Gates, D. (1968). Transpiration and leaf temperature. *Annual Review of Plant Physiology*, *19*, 211–238.

Gates, D., Hiesey, W., Milner, H., & Nobs, M. (1964). Temperatures of mimulus leaves in natural environments and in a controlled chamber. *Carnegie Inst. Wash. Yearbook*, *63*, 418–428.

Ghannoum, O., Phillips, N. G., Sears, M. A., Logan, B. A., Lewis, J. D., Conroy, J. P., & Tissue, D. T. (2010). Photosynthetic responses of two eucalypts to industrial-age changes in atmospheric [CO_2] and temperature. *Plant, Cell & Environment*, *33*, 1671–1681.

Givnish, T., & Vermeij, G. (1976). Sizes and shapes of liana leaves. *American Naturalist*, *110*, 743–778.

Givnish, T. J. (1984). Leaf and canopy adaptations in tropical forests. In E. Medina, H. A. Mooney, & C. Vázquez-Yánes (Eds.), *Physiological ecology of plants of the wet tropics: Proceedings of an international symposium held in Oxatepec and Los Tuxtlas, Mexico, June 29 to July 6, 1983* (pp. 51–84). Dordrecht: Springer, the Netherlands.

Givnish, T. J. (1987). Comparative studies of leaf form: Assessing the relative roles of selective pressures and phylogenetic constraints. *New Phytologist*, *106*, 131–160.

Grace, J. (1988). Plant response to wind. *Agriculture, Ecosystems & Environment*, *22–23*, 71–88.

Hari, P., Mäkela, A., Berninger, F., & Pohja, T. (1999). Field evidence for the optimality hypothesis of gas exchange in plants. *Functional Plant Biology*, *26*, 239–244.

Haworth, M., Gallagher, A., Sum, E., Hill-Donnelly, M., Steinthorsdottir, M., & McElwain, J. (2014). On the reconstruction of plant photosynthetic and stress physiology across the Triassic-Jurassic boundary. *Turkish Journal of Earth Sciences*, *23*, 321–329.

Helliker, B. R., & Richter, S. L. (2008). Subtropical to boreal convergence of tree-leaf temperatures. *Nature*, *454*, 511–514.

Huang, C.-W., Chu, C.-R., Hsieh, C.-I., Palmroth, S., & Katul, G. G. (2015). Wind-induced leaf transpiration. *Advances in Water Resources*, *86*, 240–255.

Jones, H. (2013). *Plants and microclimate: A quantitative approach to environmental plant physiology*. Cambridge: Cambridge University Press.

Jones, H. G. (1999). Use of thermography for quantitative studies of spatial and temporal variation of stomatal conductance over leaf surfaces. *Plant, Cell & Environment*, *22*, 1043–1055.

Katul, G., Manzoni, S., Palmroth, S., & Oren, R. (2010). A stomatal optimization theory to describe the effects of atmospheric CO_2 on leaf photosynthesis and transpiration. *Annals of Botany*, *105*, 431–442.

Katul, G. G., Ellsworth, D. S., & Lai, C.-T. (2000). Modelling assimilation and intercellular CO_2 from measured conductance: A synthesis of approaches. *Plant, Cell & Environment*, *23*, 1313–1328.

Katul, G. G., Palmroth, S., & Oren, R. (2009). Leaf stomatal responses to vapour pressure deficit under current and CO_2-enriched atmosphere explained by the economics of gas exchange. *Plant, Cell & Environment*, *32*, 968–979.

Konrad, W., Katul, G., Roth-Nebelsick, A., & Grein, M. (2017). A reduced order model to analytically infer atmospheric CO_2 concentration from stomatal and climate data. *Advances in Water Resources*, *104*, 145–157.

Lammertsma, E., De Boer, H., Dekker, S., Dilcher, D., Lotter, A., & Wagner-Cremer, F. (2011). Global CO_2 rise leads to reduced maximum stomatal conductance in Florida vegetation. *PNAS*, *108*, 4035–4040.

Leakey, A. D. B., Ainsworth, E. A., Bernacchi, C. J., Rogers, A., Long, S. P., & Ort, D. R. (2009). Elevated CO_2 effects on plant carbon, nitrogen, and water relations: Six important lessons from FACE. *Journal of Experimental Botany*, *60*, 2859–2876.

Lee, A. P., Upchurch, G., Murchie, E. H., & Lomax, B. H. (2015). Leaf energy balance modelling as a tool to infer habitat preference in the early angiosperms. *Proceedings of the Royal Society of London B: Biological Sciences*, *282*, 20143052.

Leigh, A., Sevanto, S., Close, J. D., & Nicotra, A. B. (2017). The influence of leaf size and shape on leaf thermal dynamics: Does theory hold up under natural conditions? *Plant, Cell & Environment*, *40*, 237–248.

Linacre, E. T. (1967). Further notes on a feature of leaf and air temperatures. *Archiv für Meteorologie, Geophysik Und Bioklimatologie, Serie B*, *15*, 422–436.

McElwain, J., Beerling, D., & Woodward, F. (1999). Fossil plants and global warming at the Triassic-Jurassic boundary. *Science*, *285*, 1386–1390.

Medlyn, B. E., Duursma, R. A., Eamus, D., Ellsworth, D. S., Prentice, I. C., Barton, C. V. M., … Wingate, L. (2011). Reconciling the optimal and empirical approaches to modelling stomatal conductance. *Global Change Biology*, *17*, 2134–2144.

Michaletz, S. T., Weiser, M. D., Zhou, J., Kaspari, M., Helliker, B. R., & Enquist, B. J. (2015). Plant thermoregulation: Energetics, trait-environment interactions, and carbon economics. *Trends in Ecology & Evolution*, *30*, 714–724.

Montañez, I. P., Tabor, N. J., Niemeier, D., DiMichele, W. A., Frank, T. D., Fielding, C. R., … Rygel, M. C. (2007). CO_2-forced climate and vegetation instability during late Paleozoic deglaciation. *Science*, *315*, 87–91.

Nakicenovic, N., Alcamo, J., Davis, G., de Vries, B., J., F., Gaffin, S., Gregory, K., Griibler, A., Jung, T., T., K., Lebre, E., Rovere, L., Michaelis, L., Mori, S., Morita, T., Smith, S., Swart, R., Rooijen, S., Victor, N., & Dadi, Z. (2000). *Emission scenarios. A special report of working group III of the intergovernmental panel on climate change*. Cambridge: Cambridge University Press.

Nicotra, A. B., Leigh, A., Boyce, C. K., Jones, C. S., Niklas, K. J., Royer, D. L., & Tsukaya, H. (2011). The evolution and functional significance of leaf shape in the angiosperms. *Functional Plant Biology*, *38*, 535–552.

Niinemets, Ü., Portsmuth, A., Tena, D., Tobias, M., Matesanz, S., & Valladares, F. (2007). Do we underestimate the importance of leaf size in plant economics? Disproportional scaling of support costs within the spectrum of leaf physiognomy. *Annals of Botany*, *100*, 283–303.

Nobel, P. (2005). *Physicochemical and environmental plant physiology* (3rd ed.). Amsterdam: Elsevier Academic Press.

Okajima, Y., Taneda, H., Noguchi, K., & Terashima, I. (2012). Optimum leaf size predicted by a novel leaf energy balance model incorporating dependencies of photosynthesis on light and temperature. *Ecological Research*, *27*, 333–346.

Paschalis, A., Katul, G. G., Fatichi, S., Palmroth, S., & Way, D. (2017). On the variability of the ecosystem response to elevated atmospheric CO_2 across spatial and temporal scales at the Duke Forest FACE experiment. *Agricultural and Forest Meteorology*, *232*, 367–383.

Peppe, D. J., Royer, D. L., Cariglino, B., Oliver, S. Y., Newman, S., Leight, E., … Wright, I. J. (2011). Sensitivity of leaf size and shape to climate: Global patterns and paleoclimatic applications. *New Phytologist*, *190*, 724–739.

Perri, S., Katul, G., & Molini, A. (2019). Xylem-phloem hydraulic coupling explains multiple osmoregulatory responses to salt stress. *The New Phytologist*, *224*, 644–662.

Pincebourde, S., & Casas, J. (2006). Multitrophic biophysical budgets: Thermal ecology of an intimate herbivore insect–plant interaction. *Ecological Monographs*, *76*, 175–194.

Pincebourde, S., & Woods, H. A. (2012). Climate uncertainty on leaf surfaces: The biophysics of leaf microclimates and their consequences for leaf-dwelling organisms. *Functional Ecology*, *26*, 844–853.

Prentice, I. C., Dong, N., Gleason, S. M., Maire, V., & Wright, I. J. (2014). Balancing the costs of carbon gain and water transport: Testing a new theoretical framework for plant functional ecology. *Ecology Letters*, *17*, 82–91.

Quentin, A., Crous, K., Barton, C., & Ellsworth, D. (2015). Photosynthetic enhancement by elevated CO_2 depends on seasonal temperatures for warmed and non-warmed *Eucalyptus globulus* trees. *Tree Physiology*, *35*, 1249–1263.

Reef, R., Slot, M., Motro, U., Motro, M., Motro, Y., Adame, M. F., … Winter, K. (2016). The effects of CO_2 and nutrient fertilisation on the growth and temperature response of the mangrove *Avicennia germinans*. *Photosynthesis Research*, *129*, 159–170.

Reif, F. (1974). *Fundamentals of statistical and thermal physics*. New York: McGraw-Hill.

Rockwell, F. E., Holbrook, N. M., & Stroock, A. D. (2014). The competition between liquid and vapor transport in transpiring leaves. *Plant Physiology*, *164*, 1741–1758.

Roth-Nebelsick, A. (2001). Computer-based analysis of steady-state and transient heat transfer of small-sized leaves by free and mixed convection. *Plant, Cell and Environment*, *24*, 631–640.

Schuepp, P. (1993). Tansley review no. 59. Leaf boundary layers. *New Phytologist*, *125*, 477–507.

Schymanski, S. J., & Or, D. (2016). Wind increases leaf water use efficiency. *Plant, Cell & Environment*, *39*, 1448–1459.

Smith, W. K. (1978). Temperatures of desert plants: Another perspective on the adaptability of leaf size. *Science*, *201*, 614–616.

Steinthorsdottir, M., & Vajda, V. (2015). Early Jurassic (late Pliensbachian) CO_2 concentrations based on stomatal analysis of fossil conifer leaves from eastern Australia. *Gondwana Research*, *27*, 932–939.

Voelker, S. L., Brooks, J. R., Meinzer, F. C., Anderson, R., Bader, M. K., Battipaglia, G., … Betancourt, J. L. (2016). A dynamic leaf gas-exchange strategy is conserved in woody plants under changing ambient CO_2: Evidence from carbon isotope discrimination in paleo and CO_2 enrichment studies. *Global Change Biology*, *22*, 889–902.

Vogel, S. (1968). "Sun leaves" and "shade leaves": Differences in convective heat dissipation. *Ecology*, *49*, 1203–1204.

Vogel, S. (2009). Leaves in the lowest and highest winds: Temperature, force and shape. *New Phytologist*, *183*, 13–26.

Wagner, F., Below, R., De Klerk, P., Dilcher, D. L., Joosten, H., Kürschner, W. M., & Visscher, H. (1996). A natural experiment on plant acclimation: Lifetime stomatal frequency response of an individual tree to annual atmospheric CO_2 increase. *PNAS*, *93*, 11705–11708.

Wang, D., Heckathorn, S. A., Wang, X., & Philpott, S. M. (2012). A meta-analysis of plant physiological and growth responses to temperature and elevated CO_2. *Oecologia*, *169*, 1–13.

Wing, S. L., Harrington, G. J., Smith, F. A., Bloch, J. I., Boyer, D. M., & Freeman, K. H. (2005). Transient floral change and rapid global warming at the Paleocene-Eocene boundary. *Science*, *310*, 993–996.

Zavala, J. A., Nabity, P. D., & DeLucia, E. H. (2013). An emerging understanding of mechanisms governing insect herbivory under elevated CO_2. *Annual Review of Entomology*, *58*, 79–97.

How to cite this article: Konrad W, Katul G, Roth-Nebelsick A. Leaf temperature and its dependence on atmospheric CO_2 and leaf size. *Geological Journal*. 2021;56:866–885. https://doi.org/10.1002/gj.3757

APPENDIX A

To motivate the results of Section 3.1, Equation (8) is considered in greater detail.

The special case of vanishing transpiration

First, the special case when transpiration (and thus evaporation) does not occur (e.g., when C_a is very large) is presented. This means that stomata are closed ($g = 0$), implying that leaf evaporation and the last term in Equation (8) vanish. In Figures 5 and 6, this case is represented by the dashed black lines. These lines and the solid black lines, defined by $T_l = T_a$, intersect at the temperature

$$T_{i,\infty} := \sqrt[4]{\frac{a(1+r)S_c\tau_N^{1/\sin\gamma}\sin\gamma + a_{lR}\sigma\left(T_{surr}^4 + T_{sky}^4\right)}{2e_{lR}\sigma}}, \qquad \text{(A1)}$$

which can be calculated from insertion of $g = 0$ and $T_a = T_l$ into Equation (8). All expressions under the square-root sign are necessarily positive (including $\sin\gamma$, because the angle γ that denotes the height of the sun above the horizon is restricted to the range $0 < \gamma < 90^\circ$); this guarantees the existence of $T_{i,\infty}$. Notice that $T_{i,\infty}$ only depends on the radiative properties of the leaf and can therefore serve as a reference temperature that characterizes the radiative interactions of the leaf energy balance. The $T_{i,\infty}$ is independent of w_{rel} and l_c, which

explains why it is located at the same position ($T_{i,\infty} \approx 37.9^{\circ}$C) in all sub-figures of Figures 5 and 6.

To draw further conclusions, the slope of the dashed black ($g = 0$) line is calculated. Taking the total derivative of (8) (assuming $g = 0$),

$$0 = 8e_{lR}\sigma T_l^3 dT_l + \frac{2K_a}{d_{bl}}(dT_l - dT_a) \quad \text{(A2)}$$

and then solving for dT_l/dT_a, we obtain

$$\left.\frac{dT_l}{dT_a}\right|_{g=0} = \frac{K_a}{K_a + 4d_{bl}e_{lR}\sigma T_l^3}. \quad \text{(A3)}$$

If evaporation vanishes ($g = 0$) the two results (A1) and (A3) allow the following conclusions to be drawn:

1. For $T_a < T_{i,\infty}$, leaves are warmer than the surrounding air, whereas for $T_a > T_{i,\infty}$, leaves are cooler than the air. Notice that the processes of radiation emission and heat conduction/convection alone produce this heating/cooling phenomenon, and evaporative cooling is *not* involved by definition.
2. Because all quantities in expression (A3) are positive and the numerator is smaller than the denominator, the slope of the dashed black line is positive and restricted to the (open) interval 0…1, implying that for "turned-off" leaf evaporation, T_l rises whenever T_a rises but by a smaller amount than T_a. In other words, the combination of radiative, conductive, and convective energy exchange mechanisms between leaves and atmosphere mitigates the impact of T_a-variations on T_l.

Including transpiration

If evaporation from the leaf interior is included (i.e., $g > 0$), the leaf temperature (and thus heating and cooling) is described by the coloured lines in Figures 5 and 6. They run completely below the dashed black lines related to $g = 0$, they exhibit smaller slopes than these, and they intersect the solid black line (defined by $T_a = T_l$) at lower values than $T_{i,\infty}$, implying that the temperature $T_{i,c}(C_a)$ separating the leaf heating and cooling regimes drops. The reason for all these, in terms of physics, has already been stated; since vaporization consumes heat, evaporation can transport heat only away from the leaf, that is, evaporation can only cool the leaves. In contrast, the mechanisms of conduction and convection can transport heat both ways, depending on transport direction, they can cool *or* heat the leaf.

It is instructive to relate several features depicted in Figures 5 and 6 to Equation (8).

1. Especially Figure 5 suggests quite clearly that the coloured lines approach for low temperatures the dashed black lines signifying vanishing evaporation. This makes sense: At low temperatures, assimilation yield is low, as illustrated by Figures 1b, e, and h, and plants prefer to close stomata to avoid water loss. Upon setting $g = 0$, Equation (8) reduces to the equation defining the dashed black lines.
2. With increasing leaf temperature, leaf conductance g and transpiration rate E increase (see Figures 1a,c) until g reaches its maximum value at $T_l = T_{opt}$; the maximum of $E(T_l)$ is located at a slightly higher value $T_l = T_{max}^E$ (which can be traced to the positive slope of the factor $w_l(T_l)$ in relation (6)). At $T_l = T_{max}^E$ the slopes of the coloured lines coincide with the slope of the dashed black lines. This can be understood as follows: If the assumption $g = 0$ is dropped, relation (8) implies the unrestricted version of relation (A3)

$$\frac{dT_l}{dT_a} = \frac{K_a}{K_a + 4d_{bl}e_{lR}\sigma T_l^3 + d_{bl}H_{vap}\frac{\partial E(T_l)}{\partial T_l}} \quad \text{(A4)}$$

Clearly, for $\partial E(T_l)/\partial T_l = 0$ which indicates the maximum of $E(T_l)$, this expression reduces to (A3). Thus, maximum leaf temperature reduction caused by evaporation alone occurs at $T_l = T_{max}^E$.

If leaf temperature increases beyond $T_l = T_{max}^E$ the coloured lines first approach and finally terminate at the dashed black lines. The green line in Figure 1a illustrates that this happens when the stomata close; physiologically, this is due to high leaf temperature because then (a) assimilation has declined already (as can be concluded from Figure 1b) and (b) keeping water within the plant may have become vitally important.

Relaxing the condition $g = 0$ to $g > 0$ by including evaporation as energy exchange mechanism requires a reformulation of the conclusions that were drawn at the end of section Appendix A.1:

1. For $T_a < T_{i,c}$, leaves are warmer than the surrounding air, whereas for $T_a > T_{i,c}$, leaves are cooler than the air.
2. For leaf temperature $T_l < T_{max}^E$, all quantities in expression (A4) are positive and the numerator is smaller than the denominator, the slope of the dashed black line is positive and restricted to the (open) interval 0…1. This guarantees that for $T_l < T_{max}^E$ leaf evaporation T_l rises whenever T_a rises but by a smaller amount than T_a. For $T_l > T_{max}^E$, expression $\partial E(T_l)/\partial T_l$ in the denominator of (A4) becomes negative. But if T_l obeys the condition $T_l < \sqrt[3]{-(H_{vap}/4e_{lR}\sigma)(\partial E(T_l)/\partial T_l)}$, the conclusion $dT_l < dT_a$ still applies, that is, rising air temperature is mitigated.